AFIT/GE/ENG/98J-01

A Performance Analysis of the IRIDIUM® Low Earth Orbit Satellite System

THESIS

Carl E. Fossa, Jr.

Major, USA

AFIT/GE/ENG/98J-01

Approved for public release; distribution unlimited

19980629 034

DTIC QUALITY INSPECTED 1

The views expressed in this document are those of the author and do not reflect the official policy or position of the Department of Defense or the U.S. Government.

AFIT/GE/ENG/98J-01

A Performance Analysis of The IRIDIUM® Low Earth Orbit Satellite System

THESIS

Presented to the faculty of the Graduate School of Engineering

of the Air Force Institute of Technology

Air University

In Partial Fulfillment of the

Requirements for the Degree of

Master of Science (Electrical Engineering)

Carl E. Fossa, Jr.

Major, USA

June, 1998

Approved for public release; distribution unlimited

AFIT/GE/ENG/98J-01

A Performance Analysis of
The IRIDIUM® Low Earth
Orbit Satellite System

THESIS

Presented to the faculty of the Graduate School of Engineering

of the Air Force Institute of Technology

Air University

In Partial Fulfillment of the

Requirements for the Degree of

Master of Science (Electrical Engineering)

Carl E. Fossa, Jr.

Major, USA

Richard A. Raines, Ph.D., Major, USAF
Committee Chairman

Gregg H. Gunsch, Ph.D., Lieutenant Colonel, USAF
Committee Member

Michael A. Temple, Ph.D., Major, USAF
Committee Member

Approved for public release; distribution unlimited

ACKNOWLEDGEMENTS

I would like to acknowledge the many people without whom I could not have completed this thesis. First, I would like to thank my advisor, Major Richard A. Raines. His guidance and insight throughout the research process, as well as his editing during the preparation of this document, were invaluable. Next, I would like to thank my committee members, Lieutenant Colonel Gregg H. Gunsch and Major Michael A. Temple, for their timely support to my research. Most importantly, I would like to thank my wife Susan and my daughter Christina. Their understanding, support, and love enabled me to make it through the long hours and still keep things in perspective. Thanks! I couldn't have done it without you.

Carl E. Fossa, Jr.

TABLE OF CONTENTS

ACKNOWLEDGEMENTS ..... **V**

TABLE OF CONTENTS ..... **VI**

LIST OF FIGURES ..... **X**

LIST OF TABLES ..... **XI**

ABSTRACT ..... **XIII**

CHAPTER 1 INTRODUCTION **1**

1.1 RESEARCH GOAL 1

1.2 RESEARCH MOTIVATION 1

1.3 OVERVIEW OF RESULTS 2

1.4 SUMMARY 4

CHAPTER 2 LITERATURE REVIEW **5**

2.1 INTRODUCTION 5

2.2 BRIEF HISTORY OF SATELLITE COMMUNICATIONS 6

2.3 CHARACTERISTICS OF GEO, LEO AND MEO SATELLITE SYSTEMS 7

2.4 DESIGN OF A LEO SATELLITE NETWORK 9

2.5 OVERVIEW OF PLANNED LEO SATELLITE NETWORKS 12

2.6 IRIDIUM® ISL CONNECTIVITY 14

2.7 IRIDIUM® SYSTEM CAPACITY 15

2.8 IRIDIUM® CALL PROCESSING 18

2.9 NETWORK SURVIVABILITY 21

2.10 IRIDIUM® NETWORK SURVIVABILITY 24

2.11 SUMMARY 25

CHAPTER 3 METHODOLOGY **27**

3.1 INTRODUCTION 27

3.2 METHOD OF ANALYSIS 27

3.3 SCOPE OF PROBLEM 28

3.3.1 Call Setup Procedures *28*

3.3.2 Handoff Procedures *29*

3.3.3 Number and Types of Users *29*

3.3.4 Types of Equipment Failures *30*

3.4 ASSUMPTIONS 31

3.4.1 Packet Size and Data Structures *31*

3.4.2 Packet Arrival Rate *33*

3.4.3 Satellite Processing Delay *33*

3.4.4 Loading Levels *34*

3.4.5 Traffic Distribution *36*

3.4.6 Routing Algorithm *38*

3.4.7 ISL Establishment *39*

3.4.8 Delay Calculations *40*

3.4.9 Network Access *43*

3.4.10 Queue Size *43*

3.5 MODEL DESIGN 44

3.6 SIMULATION SCALING 48

3.7 MODEL VERIFICATION AND VALIDATION 50

3.7.1 Verification *51*

3.7.2 Validation *53*

3.8 ALGORITHMIC SELECTION OF FAILED SATELLITES 54

3.9 INPUT PARAMETERS 56

3.9.1 Loading Level *56*

3.9.2 Number of Satellites Removed *56*

3.9.3 Traffic Distribution *57*

3.10 PERFORMANCE METRICS 57

3.10.1 End-to-End Delay *57*

3.10.2 Packet Rejection Rate *57*

3.10.3 Average Number of Visible Satellites *57*

3.10.4 Cumulative Outage Time *58*

3.10.5 Maximum Continuous Outage Time *59*

3.11 SUMMARY 59

CHAPTER 4 ANALYSIS 60

4.1 INTRODUCTION 60

4.2 STATISTICAL ACCURACY 60

4.3 DELAY TEST SCENARIOS 62

4.3.1 Uniform Distribution Low Load *63*

4.3.2 Uniform Distribution Medium Load *63*

4.3.3 Uniform Distribution High Load *63*

4.3.4 Non-uniform Distribution Low Load *64*

4.3.5 Non-Uniform Distribution Medium Load *64*

4.4 ANALYSIS OF DELAY PERFORMANCE METRICS 65

4.4.1 Delay Analysis *65*

4.4.2 Packet Rejection Analysis *69*

4.5 ANALYSIS OF DELAY TEST SCENARIOS 71

4.5.1 Uniform Distribution Low Load *72*

4.5.2 Uniform Distribution Medium Load *73*

4.5.3 Uniform Distribution High Load *74*

4.5.4 Non-uniform Distribution Low Load *75*

4.5.5 Non-Uniform Distribution Medium Load *76*

4.6 NETWORK ACCESS TEST SCENARIOS 78

4.6.1 Equatorial City *78*

4.6.2 North American City *79*

4.7 ANALYSIS OF NETWORK ACCESS PERFORMANCE METRICS 79

4.7.1 Analysis of Average Number of Visible Satellites *79*

4.7.2 Analysis of Cumulative Outage Time *80*

4.7.3 Analysis of Maximum Continuous Outage Time *81*

4.8 ANALYSIS OF NETWORK ACCESS TEST SCENARIOS 82

4.8.1 Equatorial City *83*

4.8.2 North American City *84*

4.9 SUMMARY OF ANALYSIS 85

CHAPTER 5 CONCLUSIONS AND RECOMMENDATIONS 87

5.1 RESTATEMENT OF RESEARCH GOAL 87

5.2 CONCLUSIONS 87

5.3 SIGNIFICANT RESULTS OF RESEARCH 88

5.4 RECOMMENDATIONS FOR FUTURE RESEARCH 89

APPENDIX 87

BIBLIOGRAPHY 97

VITA 99

LIST OF FIGURES

FIGURE 1: SATELLITE COVERAGE AREA 10

FIGURE 2: IRIDIUM® TDMA FRAME STRUCTURE 16

FIGURE 3: IRIDIUM® FDMA SCHEME 16

FIGURE 4: IRIDIUM® FREQUENCY REUSE SCHEME 18

FIGURE 5: SIMPLE ONE CONNECTED NETWORK 22

FIGURE 6: SIMPLE TWO CONNECTED NETWORK 23

FIGURE 7: TYPICAL DELAY VS. LOADING CURVE 35

FIGURE 8: MAXIMUM END-TO-END DELAY 44

FIGURE 9: SIMULATION TOP LEVEL 45

FIGURE 10: DELAY FOR UNIFORM DISTRIBUTION AND FULL CONSTELLATION 66

FIGURE 11: DELAY FOR UNIFORM DISTRIBUTION AND SEVEN NON--OPERATIONAL SATELLITES 67

FIGURE 12: DELAY FROM KANSAS CITY TO DHAHRAN 68

FIGURE 13: DELAY FROM KANSAS CITY TO BERLIN 69

FIGURE 14: PACKET REJECTION RATE FOR EACH SCENARIO 70

FIGURE 15: DELAY KANSAS CITY TO OTHER EARTH STATIONS UNIFORM LOW LOAD SCENARIO 72

FIGURE 16: DELAY FROM KANSAS CITY TO OTHER EARTH STATIONS UNIFORM MEDIUM LOAD 73

FIGURE 17: DELAY FROM KANSAS CITY TO OTHER EARTH STATIONS UNIFORM HIGH LOAD 75

FIGURE 18: DELAY FROM KANSAS CITY TO OTHER EARTH STATIONS NON-UNIFORM LOW LOAD 76

FIGURE 19: DELAY FROM KANSAS CITY TO OTHER EARTH STATIONS NON-UNIFORM MEDIUM LOAD 77

FIGURE 20: AVERAGE NUMBER OF VISIBLE SATELLITES BY SCENARIO 80

FIGURE 21: CUMULATIVE OUTAGE TIME BY SCENARIO 81

FIGURE 22: MAXIMUM CONTINUOUS OUTAGE TIME BY SCENARIO 82

FIGURE 23: PERCENT OF TIME SATELLITES ARE VISIBLE FROM EQUATOR 83

FIGURE 24: PERCENT OF TIME SATELLITES ARE VISIBLE FROM KANSAS CITY 84

LIST OF TABLES

TABLE 1: COMPARISON OF GLOBALSTAR AND IRIDIUM® 13

TABLE 2: EARTH STATION DATA 30

TABLE 3: EARTH STATION LOADING LEVELS 34

TABLE 4: UNIFORM TRAFFIC DISTRIBUTION 36

TABLE 5: NON-UNIFORM TRAFFIC DISTRIBUTION LOW LOAD 37

TABLE 6: NON-UNIFORM LOW LOADING LEVELS 37

TABLE 7: NON-UNIFORM TRAFFIC DISTRIBUTION MEDIUM LOAD 38

TABLE 8: NON-UNIFORM MEDIUM LOADING LEVELS 38

TABLE 9: DATA STRUCTURE FIELDS 47

TABLE 10: 95% CI FOR UNIFORM-LOW-LOAD WITH A FULL SATELLITE CONSTELLATION 62

TABLE 11: 95% CI FOR NON-UNIFORM-MEDIUM-LOAD AND SEVEN NON-OPERATIONAL SATELLITES 62

TABLE 12: NETWORK ACCESS RESULTS FOR EQUATORIAL CITY SCENARIO 83

TABLE 13: NETWORK ACCESS RESULTS FOR NORTH AMERICAN CITY SCENARIO 85

TABLE 14: RESULTS FOR UNIFORM LOW LOAD WITH THREE NON-OPERATIONAL SATELLITES 90

TABLE 15: RESULTS FOR UNIFORM LOW LOAD WITH FIVE NON-OPERATIONAL SATELLITES 90

TABLE 16: RESULTS FOR UNIFORM LOW LOAD WITH SEVEN NON-OPERATIONAL SATELLITES 91

TABLE 17: RESULTS FOR UNIFORM MEDIUM LOAD WITH A FULL SATELLITE CONSTELLATION 91

TABLE 18: RESULTS FOR UNIFORM MEDIUM LOAD WITH THREE NON-OPERATIONAL SATELLITES 91

TABLE 19: RESULTS FOR UNIFORM MEDIUM LOAD WITH FIVE NON-OPERATIONAL SATELLITES 92

TABLE 20: RESULTS FOR UNIFORM MEDIUM LOAD WITH SEVEN NON-OPERATIONAL SATELLITES 92

TABLE 21: RESULTS FOR UNIFORM HIGH LOAD WITH A FULL SATELLITE CONSTELLATION 92

TABLE 22: RESULTS FOR UNIFORM HIGH LOAD WITH THREE NON-OPERATIONAL SATELLITES 93

TABLE 23: RESULTS FOR UNIFORM HIGH LOAD WITH FIVE NON-OPERATIONAL SATELLITES 93

TABLE 24: RESULTS FOR UNIFORM HIGH LOAD WITH SEVEN NON-OPERATIONAL SATELLITES 93

TABLE 25: RESULTS FOR NON-UNIFORM LOW LOAD WITH A FULL SATELLITE CONSTELLATION 94

TABLE 26: RESULTS FOR NON-UNIFORM LOW LOAD WITH THREE NON-OPERATIONAL SATELLITES 94

TABLE 27: RESULTS FOR NON-UNIFORM LOW LOAD WITH FIVE NON-OPERATIONAL SATELLITES 94

TABLE 28: RESULTS FOR NON-UNIFORM LOW LOAD WITH SEVEN NON-OPERATIONAL SATELLITES 95

TABLE 29: RESULTS FOR NON-UNIFORM MEDIUM LOAD WITH A FULL SATELLITE CONSTELLATION 95

TABLE 30: RESULTS FOR NON-UNIFORM MEDIUM LOAD WITH THREE NON-OPERATIONAL SATELLITES 95

TABLE 31: RESULTS FOR NON-UNIFORM MEDIUM LOAD WITH FIVE NON-OPERATIONAL SATELLITES 96

ABSTRACT

This thesis provides a performance evaluation of the IRIDIUM® Low Earth Orbit Satellite system. It examines the system's ability to meet real-time communications constraints with a degraded satellite constellation. The analysis is conducted via computer simulation. The simulation is run at low, medium and high loading levels with both uniform and non-uniform traffic distributions. An algorithmic approach is used to select critical satellites to remove from the constellation. Each combination of loading level and traffic distribution is analyzed with zero, three, five, and seven non-operational satellites. The measured outputs are end-to-end packet delay and packet rejection rate. In addition to the delay analysis, a user's ability to access the network with a degraded satellite constellation is evaluated. The average number of visible satellites, cumulative outage time, and maximum continuous outage time are analyzed for both an Equatorial city and a North American city. The results demonstrate that the IRIDIUM® network is capable of meeting real-time communication requirements with several non-operational satellites. Both the high loading level and the non-uniform traffic distribution have a significant effect on the network's performance. The analysis of both network delay performance and network access provides a good measure of the overall network performance with a degraded satellite constellation.

CHAPTER 1

INTRODUCTION

1.1 Research Goal

The goal of this research is to assess the IRIDIUM® Low Earth Orbit (LEO) satellite network's capability to provide real-time communications with a degraded satellite constellation.

1.2 Research Motivation

This thesis provides a performance analysis of the IRIDIUM® LEO satellite system with a degraded satellite constellation. The concept of LEO satellite communications (SATCOM) is relatively new and provides many interesting research opportunities. This is exemplified by the fact that several commercial organizations are currently developing LEO SATCOM systems. Two such systems, IRIDIUM® and GLOBALSTAR, are scheduled to be operational in 1998. They will both provide worldwide voice, data, facsimile and paging services. The IRIDIUM® system will be the first commercial system to use inter-satellite communication links. In effect, this will form a network in the sky with satellites acting as switching nodes. Subscribers will have a single telephone number and a handset similar in size to a cellular telephone. These LEO satellite networks are intended to augment the existing terrestrial and cellular networks.

My personal interest in this area of research is motivated in part by my experience as a U.S. Army Signal Officer. I have spent the last ten years working with a variety of military communications systems. There have been two noticeable trends in military

communications over the past decade. The first is the movement toward mobile communications systems. This is exemplified by the Army's fielding of Mobile Subscriber Equipment (MSE) in the late 1980s. MSE is an area communications system that provides voice, data, and facsimile service to tactical military users. One of the key features of MSE is a user's ability to keep the same telephone number as he moves around the battlefield. MSE also provides wireless communications, similar to cellular telephone service, through the use of Radio Access Units (RAUs). The second trend in military communications is the movement toward commercial equipment standards. In the past, military communications systems were stand-alone systems. Today, they are designed to interface with both commercial systems and other military systems. The military use of commercial technology has become so common that the military has adopted an acronym for it, Commercial Off The Shelf (COTS) equipment. The commercial LEO satellite technology currently under development appears to have good potential for future integration into military communications systems. A survivability analysis of one of these systems will provide insight into the feasibility of integrating commercial LEO satellite technology into military communications systems.

1.3 Overview of Results

This research began as a follow on to Douglas Stenger's work in the area of IRIDIUM® survivability analysis [Ste96]. Stenger's research focused on the performance of different routing algorithms in a faulting IRIDIUM® network. Stenger's work examined the Dijkstra, Extended Bellman Ford, and DARTING routing algorithms with different numbers of non-operational satellites and varying loading levels. Stenger concluded that the IRIDIUM® network was highly survivable. His results showed

acceptable end-to-end delays for all routing algorithms with as many as 45% of the satellites removed from the IRIDIUM® constellation. However, Stenger's research had three significant areas that could be improved. First, long simulation run times limited Stenger's research to two transmitting earth stations and an 11% traffic load. Second, he did not use an algorithmic approach to select which satellites to remove from the constellation. Finally, he did not analyze the effect that removing satellites from the constellation has on a user's ability to connect to the network. This research focused on improving the analysis of the IRIDIUM® system in all three of these areas.

This research improved upon Stenger's work both by increasing the loading level and by algorithmically selecting which satellites to remove from the constellation. It analyzed low, medium, and high traffic loading levels of 50%, 83% and 100% respectively. The algorithm selected the most loaded satellites to remove from the constellation. This research also increased the number of transmitting earth stations to seven. Using more than two earth stations allowed the analysis of both uniform and non-uniform traffic distributions. With a low loading level and a uniform traffic distribution the system had end-to-end delays below 400-ms and packet rejection rates below 1% with up to seven non-operational satellites. This was consistent with Stenger's previous work. At a high loading level with a uniform traffic distribution the network experienced packet rejection rates above 1% with only three non-operational satellites. A medium loading level with a non-uniform traffic distribution produced packet rejection rates above 3% with a full satellite constellation. The results of this research demonstrated that the loading level, the traffic distribution, and the algorithmic selection of satellites had a

significant effect on the IRIDIUM® system's capability to perform with a degraded satellite constellation.

This research also improved upon Stenger's work by analyzing the ability to access the IRIDIUM® network with a degraded satellite constellation. The results demonstrated that a typical North American city exceeded both the benchmark of 12.04-minutes maximum continuous outage time and the benchmark of 55.41-minutes of cumulative outage time with five non-operational satellites. So even though the IRIDIUM® system had acceptable delay performance with a low loading level and seven non-operational satellites, the ability to access the network with these failed satellites was not acceptable. The combination of end-to-end delay analysis and network access analysis provided a more complete assessment of the IRIDIUM® system.

1.4 Summary

This chapter has defined the goal of this research and provided a brief summary of the motivation to study LEO satellite network performance. Chapter 2 presents a review of the current literature in the area of LEO satellites and network survivability. This includes previous work in IRIDIUM® network survivability. Chapter 3 explains the methodology used to analyze the performance of the IRIDIUM® system and discusses the design and testing of the simulation model. Chapter 4 provides the results of the simulation runs and analyzes these results. Chapter 5 contains conclusions from the research and recommendations for additional research in the area of LEO satellite networks.

CHAPTER 2

LITERATURE REVIEW

2.1 Introduction

This goal of this chapter is to provide the theoretical background necessary to model and analyze the performance of the IRIDIUM® system. There is currently a renewed interest in the development of a LEO satellite system that provides worldwide personal communication services (PCS). PCS devices, such as pagers and cellular telephones, were considered luxury items as recently as 1990. However, over the past several years the number of PCS devices in use has increased drastically. In July, 1993 there were over 25 million cellular phones worldwide, and recent estimates indicate this number will increase to over 100 million by the year 2000 [Ana95]. Technological advances have made worldwide mobile communications a realistic possibility. Several commercial consortiums are planning LEO satellite networks that will be in service before the year 2000 [Bru96]. These networks will provide a range of worldwide services including voice, data, facsimile and paging. This chapter presents an overview of these systems focusing primarily on the IRIDIUM® LEO satellite network.

The chapter begins with a brief history of satellite communications in Section 2.2. Section 2.3 introduces three categories of satellite networks, the geostationary earth orbit (GEO), medium earth orbit (MEO) and LEO. The characteristics, advantages, and disadvantages of each type of network are discussed. In Section 2.4, the design of a LEO satellite network is discussed based upon number of satellites, altitude of orbits, and location of switching nodes. Section 2.5 compares the characteristics of GLOBALSTAR

and IRIDIUM®, two commercial LEO networks that are currently under development. In Section 2.6, the establishment of inter-satellite links (ISLs) is discussed with respect to antenna pointing angles between satellites. The IRIDIUM® system capacity is discussed in Section 2.7. In Section 2.8, the process of call establishment and setup in the IRIDIUM® network is explained. This includes a discussion of both the format of an IRIDIUM® phone number and the function of IRIDIUM® gateways. Section 2.9 presents an overview of network survivability and Section 2.10 discusses previous work in the area of IRIDIUM® network survivability analysis.

2.2 Brief History of Satellite Communications

A satellite communication system is basically a microwave radio system with a single repeater. Ground stations transmit signals to the satellite via the uplink. The satellite transponder serves as the repeater, and retransmits the signals over the downlink. The satellite downlink is broadcast in the satellite coverage area. The first communication satellite was placed in orbit in 1958 [Saa94]. The first commercial GEO satellite, INTELSAT I, was launched in 1965. It used 50-MHz of bandwidth and provided 240 voice circuits between the United States and Europe. INTELSAT I utilized non-linear, hard limited transponders and only two ground stations could access the satellite simultaneously. INTELSAT II and III used travelling wave tubes operating in the linear region, which improved multiple access to the satellite. The current version, INTELSAT VI, was launched in 1989. It uses 33-GHz of bandwidth and simultaneously carries 120,000 voice channels and 3 television channels [Skl88]. The first generation of GEO satellite mobile communications began with INMARSAT-A in 1982 [Com93, Ana95]. The ship-based user stations had a 40 W transmitter and a 1.2-meter dish

antenna [Com93]. The current version, INMARSAT-M, became operational in 1993 and has suitcase-sized user terminals [Ana95]. Today, satellite communication is a vital part of international business and global communications.

2.3 Characteristics of GEO, LEO and MEO Satellite Systems

Existing satellite communication systems primarily use GEO satellites with an altitude of approximately 35,800-km [Com93, Vat95]. GEO satellite systems have the advantage of allowing full earth coverage, below 70 degrees latitude, with as few as three satellites. GEO satellites are also easy to track since they appear stationary with respect to a point on earth. However, GEO satellite systems have the disadvantages of high propagation delay and high propagation loss. The one way propagation delay of a GEO satellite system is approximately 120-ms. The propagation loss for a radio frequency signal is directly proportional to the square of the path distance. This is described in Equation 1 where λ equals wavelength and d equals path distance:

$$Ls = \left(\frac{4\pi d}{\lambda} \right)^2 \tag{1}$$

It is necessary to use either a high power transmitter or a large antenna to compensate for the propagation loss associated with transmitting over a distance of 35,800-km. This increases the size and weight of ground satellite stations and makes hand-held user terminals impractical. Another disadvantage of GEO satellite systems is that they orbit above the Van Allen belt. As a result, the satellites must be hardened to protect the electronics. This increases the weight and fabrication cost of the satellite.

LEO satellites orbit at an altitude between 500-km and 1,500-km and move with respect to a point on earth. The primary advantages of LEO satellites are a lower

propagation delay, lower required transmit power, and polar coverage. The one-way propagation delay of a LEO satellite system is between 1.7-ms and 5-ms. The propagation loss that results from transmitting 500-km to 1,500-km is low enough to allow hand-held battery powered user terminals. LEO satellite networks use numerous satellites in near-polar orbits to provide worldwide coverage including the polar regions. Also, since the altitude of LEO satellites is below the Van Allen belt they do not have to be hardened. This means that the satellites are lighter, cheaper to fabricate, and easier to deploy. The most significant disadvantages of LEO satellites are the large number of satellites required for worldwide coverage, and the difficult task of tracking satellites that move with respect to ground stations.

MEO satellites orbit at an altitude between 5,000-km and 20,000-km and offer a compromise between GEO and LEO satellites. A MEO satellite system has a lower propagation delay than a GEO satellite system, and has both fewer satellites and easier tracking than a LEO satellite system. The one way propagation delay of a MEO satellite system is between 16.7-ms and 66.7-ms. This is low enough that a signal between two users can traverse two complete MEO satellite links and remain within CCITT Recommendations G.114 for end-to-end delay [Vat95]. MEO satellites provide worldwide coverage with as few as 10 satellites. MEO satellites are visible to an earth station for approximately two hours, while LEO satellites are visible for about ten minutes. This simplifies the tasks of tracking the satellites and handing off calls between satellites. The main disadvantage of MEO satellites is that the propagation loss is too large to make hand-held user terminals practical. Odyssey is a proposed commercial MEO system that will have four satellites in each of three orbital planes for a total of 12

satellites. The orbits will have an altitude of 10,600-km and an inclination of 55 degrees relative to the equator. Although MEO satellites are not well suited for PCS, the long overhead periods could prove useful in maritime applications where there is less of a requirement for small terminals.

2.4 Design of a LEO Satellite Network

There are different approaches to designing a LEO satellite network that vary based upon the type of service provided, the satellite constellation, and the network connectivity. The type of service provided by a LEO satellite network is classified by the bandwidth and delay requirements. Big LEO systems will provide a higher bandwidth and lower delay service that is suitable for voice applications. Little LEO systems will provide a lower bandwidth and higher delay service that can support facsimile, electronic mail, and paging services. Most current commercial designs are Big LEO systems that plan to offer voice, facsimile, and paging services.

The design of a LEO satellite constellation involves selecting the number of satellites, the altitude of the orbits, the minimum elevation angle, the number of orbits, and the number of spot beams in a satellite footprint. The number of satellites is selected to provide full earth coverage based on each satellite's coverage area. The coverage area of a single satellite, depicted in Figure 1, is given by Equation 2 where R_e is the radius of the earth and θ is the earth central angle [Gag84].

$$A = 2\pi R_e^2 \left(1 - \cos\theta\right) \tag{2}$$

The earth central angle θ is calculated using Equation 3 where R_e is the radius of the earth, E is the minimum elevation angle, and h is the satellite altitude [Gag84].

$$\theta = \left[\cos^{-1}\left(\frac{R_e \cos E}{R_e + h}\right)\right] - E \tag{3}$$

The altitude of the satellite and the minimum elevation angle determine the size of the coverage area with a higher altitude and lower elevation angle resulting in a larger coverage area. In general, the number of satellites required for global coverage is inversely proportional to the satellite altitude. The propagation distance to the satellite is also a function of the satellite altitude. The minimum propagation distance occurs when the satellite is directly overhead and is equal to the satellite altitude. The maximum propagation distance, depicted as *d* in Figure 1, is calculated using Equation 4.

$$d = (R_e + h)\sqrt{1 + \frac{R_e}{R_e + h} - 2\frac{R_e}{R_e + h}\cos(\theta)} \tag{4}$$

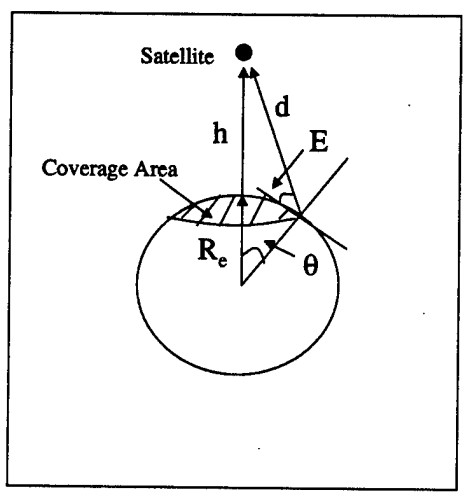

Figure 1: Satellite Coverage Area

The number of satellites, *S*, are arranged in *m* orbits with *n* satellites equally spaced in each orbit according to the equation $S = m \times n$. The *m* orbits are spaced approximately *180/m* degrees apart. A satellite with higher altitude has a larger coverage area, but its

transmitted power is effectively spread across the area of coverage. Therefore, a higher altitude satellite requires a higher transmitted power in order for a user to have the same received signal power. The underlying design trade-off is between the number of satellites required and the transmitter power required on the satellite. An approach to reducing the power required on the satellite is to use multiple spot beam antennas. Each spot beam focuses its power in a small portion of the footprint and uses a lower transmitter power. Another aspect of the satellite constellation that is dependent on the satellite altitude is the velocity of the satellite relative to the earth. The velocity of a LEO satellite relative to the earth is given by Equation 5 where ω is the earth angular rotation speed, R_g is the GEO satellite orbit radius, and R_l is the LEO satellite orbit radius [Gan93].

$$V_l = \frac{\omega R_g^{3/2}}{\sqrt{R_l}} \tag{5}$$

The angular rotation of the earth is calculated as 0.2618-radians/hour using Equation 6.

$$\omega = \frac{2\pi \, radians}{24 \, hours} = 0.2618 \, radians / hour \tag{6}$$

Lower satellites have a higher velocity relative to earth and are visible for a shorter amount of time. This contributes to the difficulty in tracking the satellites.

There are currently two design approaches for connectivity in a LEO satellite network. These approaches depend upon whether the satellites serve as repeaters, or if they have onboard switching equipment. A "bent pipe" architecture uses satellites that serve as repeaters. A mobile user's transmitted signal is received and retransmitted by the satellite to a gateway in the same satellite footprint. The switch used to process the call is

located at the gateway. Locating the switches at the gateways simplifies the satellite design and allows for future upgrades to the switching equipment. This type of system requires a gateway in each satellite footprint in order to interface mobile users. Satellites with onboard switching equipment are able to use inter-satellite links (ISLs) to route calls. A mobile user's transmitted signal is routed through several satellites and downlinked to either a regional gateway or another mobile user. This creates a network in the sky and allows the use of large regional gateways instead of gateways in each satellite footprint. However, the switching equipment increases the weight of the satellites. The heavier satellites are more expensive to launch and have a shorter life span. Placing the switching equipment on the satellite requires very precise orbits for tracking of ISLs. It also means that new satellites must be launched to upgrade switching equipment.

2.5 Overview of Planned LEO Satellite Networks

Two proposed commercial LEO systems that use different constellation and connectivity designs are GLOBALSTAR and IRIDIUM®. The characteristics of these networks are summarized in Table 1. The GLOBALSTAR network is being developed by a group of companies that includes Loral, QUALCOMM, SS/L, AirTouch and numerous others [Com93]. The network will provide voice, data, paging and facsimile services. The satellite constellation has 48 satellites in 8 orbits at an altitude of 1,400-km. The network topology uses "bent pipe" transmission links and switching at the gateways. The technology needed to manufacture satellites that perform as relays is widely used in GEO satellites. As such, the GLOBALSTAR LEO network is being developed around existing technology and is a relatively conservative design.

Table 1: Comparison of GLOBALSTAR and IRIDIUM®

	GLOBALSTAR	IRIDIUM®
Altitude (Km)	1400	780
No. of Satellites	48	66
No. of Orbits	8	6
Inclination of Orbits (deg)	52	86
No. of Spot Beams	16	48
Switching	Gateway	Satellite
Link Type	Bent Pipe	ISL
Weight (lbs.)	510	1516
Life Span (years)	7.5	5 to 7
Modulation	CDMA	TDMA/FDMA

In the GLOBALSTAR network, user uplinks will utilize the frequency range of 1.610 to 1.625-GHz and user downlinks will utilize the frequency range of 2.4835 to 2.500-GHz [Com93]. A GLOBALSTAR satellite will have 2,800 full duplex circuits [Com93]. The fact that GLOBALSTAR uses Code Division Multiple Access (CDMA) modulation is technically significant because the consortium plans to have one hand-held device for cellular and satellite communications. Many existing cellular telephone networks use CDMA technology, and it is advantageous to use the same modulation for both the cellular and satellite portions of the hand-held device. The first GLOBALSTAR satellites are scheduled to be launched in early 1998.

The IRIDIUM® system is being developed by an international consortium of telecommunications companies that includes Motorola, Raytheon, Siemens, Telesat and Bechtel [Bru96, Com93]. Like GLOBALSTAR, it will offer voice, data, paging and facsimile services. The IRIDIUM® satellite constellation consists of six orbital planes with eleven satellites in each plane for a total of 66 LEO satellites. The satellites are arranged using the Adams/Rider circular polar constellation [Kel96, Ada87]. The

satellites are in a circular orbit at an altitude of approximately 780-km and at an inclination of 86.4 degrees. Orbital planes one and six are counter-rotating and are separated by approximately 22 degrees. The remaining orbital planes are co-rotating and are separated by approximately 31.6 degrees [Hub97]. The most significant aspect of IRIDIUM® is that it is currently the only commercial network that plans to use both ISLs and switching equipment on the satellites. The IRIDIUM® uplinks and downlinks will use a combination of Time Division Multiple Access (TDMA) and Frequency Division Multiple Access (FDMA) for multiple access to the satellite. The TDMA frame is 90-ms long and accommodates four 50-kbps user accesses per frame [Hub97]. The TDMA scheme allows the same frequencies to be used on both the uplink and downlink without interference. In the IRIDIUM® network, user uplinks and downlinks will both utilize the frequency range of 1.616 to 1.6265-GHz. An IRIDIUM® satellite will have 3840 full duplex circuits. The IRIDIUM® network is an aggressive design using untested technology. However, the aggressive design has potential benefits in area of coverage. The IRIDIUM® network allows two mobile subscribers to communicate without the call going through a gateway. In addition, the network offers potential advantages for communication over water where the proper placement of gateways is difficult. The IRIDIUM® network is scheduled to be operational in late 1998.

2.6 IRIDIUM® ISL Connectivity

The IRIDIUM® network will have up to four ISLs for each satellite operating at a data rate of 25-Mbps in the 22.55 to 23.55-GHz frequency range [Com93, Hub97]. The length of these links is approximately 4,000-km. Two of these links will be intra-orbital links to the forward and aft adjacent satellites in the same orbital plane. There will also

be up to two inter-orbital links, one each to the two adjacent orbital planes. The horizontal pointing angle between two satellites in adjacent orbital planes, using a reference of zero degrees parallel to the equator, varies between approximately ±65 degrees over one orbital period [Kel96, Wer95]. This angle varies most slowly over the equator where satellites in adjacent orbits are the most separated, and it varies most rapidly over the poles where the orbits cross. The variation in horizontal azimuth between satellites makes antenna steering necessary to maintain inter-orbital links. Even with antenna steering, it would be very difficult to maintain inter-orbital links at higher latitudes where the azimuth varies rapidly. An approach to maintaining inter-orbital links is to select a nominal horizontal azimuth close to that between satellites over the equator. Then the antenna is designed to have a steering range that allows inter-orbital links at lower latitudes where the horizontal azimuth changes more slowly. A nominal horizontal azimuth of ± 45 to 50 degrees with an antenna steering range of 30 to 45 degrees is sufficient to maintain inter-orbital links between latitudes of 50 to 60 degrees north and south [Kel96, Wer95]. Although the actual characteristics of the ISL antennas on IRIDIUM® satellites are not known, this approach is reasonable since it allows inter-orbital ISLs over the most populated regions of the earth.

2.7 IRIDIUM® System Capacity

The IRIDIUM® system uses a combination of TDMA and FDMA. The TDMA frame is 90-ms long and it contains four full duplex user channels at a burst data rate of 50-kbps [Com93, Hub97, Gea96]. The IRIDIUM® TDMA frame structure is shown in Figure 2. The four full duplex channels consist of four uplink time slots and four

downlink time slots. The IRIDIUM® system will support full duplex voice channels at 4,800-bps and half duplex data channels at 2,400-bps [Com93].

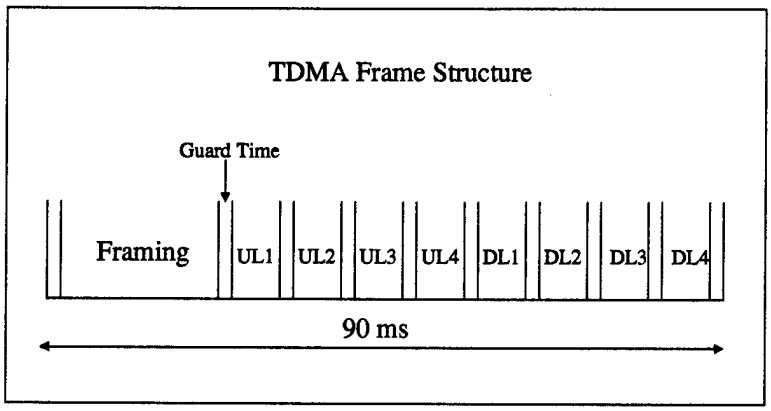

Figure 2: IRIDIUM® TDMA Frame Structure

IRIDIUM® uses frequencies in the L-band of 1.616 to 1.6265-GHz for the user's uplink and downlink with the satellites [Com93, Hub97]. This gives the system 10.5-MHz of bandwidth. The IRIDIUM® FDMA scheme divides the available bandwidth into 240 channels of 41.67-kHz for a total of 10-MHz [Gea96]. This leaves 500-kHz of bandwidth for guard bands, which amounts to approximately 2-kHz of guard band between channels. The IRIDIUM® FDMA scheme is shown in Figure 3.

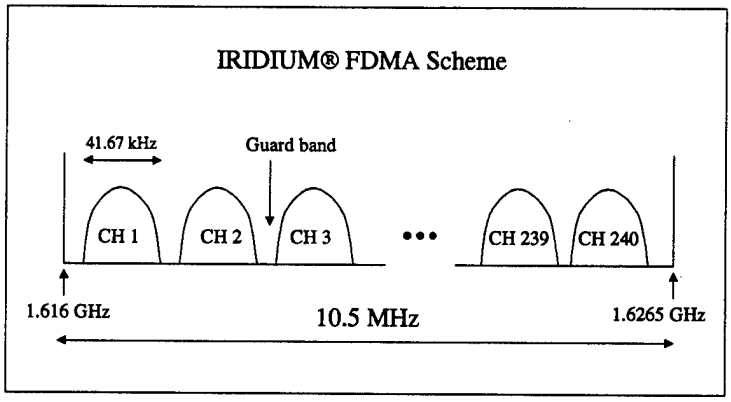

Figure 3: IRIDIUM® FDMA Scheme

The IRIDIUM® network utilizes multiple spot beams on each satellite that divide the satellite footprint into smaller cells. Each IRIDIUM® satellite has three phased array

antennas with 16 spot beams for a total of 48 spot beams on the satellite [Com93, Hub97]. A spot beam, like a cell in a typical cellular network, is assigned a fraction of the available frequency channels. Frequency channels can be reused throughout the network by assigning them to cells that are far enough apart to minimize co-channel interference. The IRIDIUM® network uses a frequency reuse factor of 12, which means there are 12 cells in each cluster [Hub97]. As shown in Equation 7, this equates to 20 frequency channels per cell.

$$\frac{240\ channels}{12\ cells} = 20\ channels\ per\ cell \tag{7}$$

The frequency reuse factor is described by Equation 8 where I and J are non-negative integers.

$$N = I^2 + I \cdot J + J^2 \tag{8}$$

Cells that use the same frequency channels are found by starting in the center of a cell, moving I cells across cell sides, turning 60 degrees, and moving J cells. This is illustrated in Figure 4 where cells with the same letter use the same frequency channels.

The capacity of the IRIDIUM® network can be calculated by multiplying the number of possible users per cell by the number of active cells in the network. Each cell has four TDMA channels on 20 frequencies for a total of 80 possible users. The IRIDIUM® network has 48 cells on each of the 66 satellites for a total of 3,168 cells. Since some of the spot beams will overlap, especially near the poles, only 2,150 of the possible 3,168 cells will be active at once [Hub97]. The remaining spot beams will be turned off to conserve power. The network has 80 users in 2,150 active cells for a total network capacity of 172,000 simultaneous users.

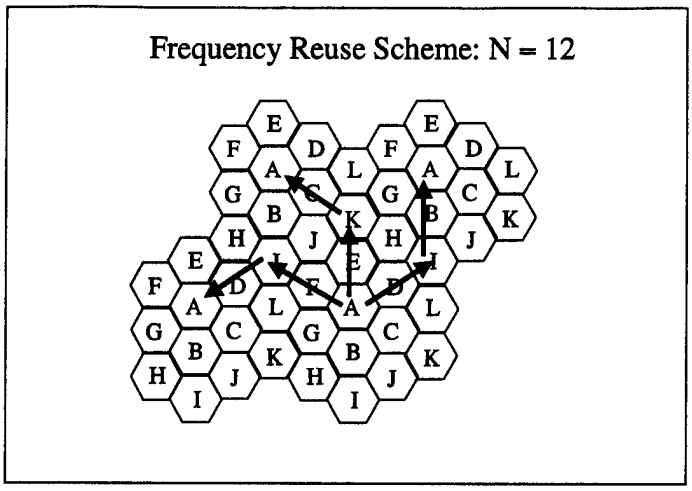

Figure 4: IRIDIUM® Frequency Reuse Scheme

This maximum network capacity implies that the users are distributed across all the active beams. The calculation does not take into account the fact that many of the satellites will be over the ocean or other low populated areas. Each satellite has 80 users in 48 cells for a maximum of 3,840 simultaneous users per satellite. The size of an IRIDIUM® satellite footprint is calculated as 15,299,900-km^2 using Equations 2 and 3. Each IRIDIUM® satellite is therefore capable of supporting an average of one simultaneous user per 3,984-km^2 of coverage area.

2.8 IRIDIUM® Call Processing

The IRIDIUM® system will allow users to roam worldwide and still utilize a single subscriber number. To accomplish this, each user will have a home gateway that normally provides his service. The gateways in this system will be regional and will support large geographical areas. For example, a single gateway will service North America. The gateways serve as the interface to the Public Switched Telephone Network (PSTN). They also perform the functions of call setup, call location and billing. The

gateway must maintain a database of subscriber profiles as well as subscriber locations. This register is called the Home Location Register (HLR).

An IRIDIUM® subscriber will be uniquely identified by three numbers, the Mobile Subscriber Integrated Services Digital Network Number (MSISDN), the Temporary Mobile Subscriber Identification (TMSI), and the Iridium Mobile Subscriber Identity (IMSI) [Hub97]. The MSISDN is the telephone number of an IRIDIUM® subscriber. The MSISDN is five digits long, and makes up part of the twelve-digit number dialed to reach a subscriber. The first field of the twelve-digit number is the four-digit country code. This is similar to the country codes used now with the PSTN. The IRIDIUM® network will have its own country codes and is currently assigned the codes 8816 and 8817 [Hub97]. The second field of the number is a three digit geographical code. This code will be used to identify a user's home country in regions where one gateway services more than one country. The third and final field of the number is the MSISDN. The TMSI is a temporary number that is transmitted over the network during call setup. This number is changed periodically to protect subscriber confidentiality [Hub97]. The IMSI is a permanent number stored on a credit card sized module that the subscriber inserts into the mobile phone unit. This number contains information that allows a gateway to uniquely identify a user and determine his home gateway.

The IRIDIUM® network must track a user's location as he roams in order to set up calls. When a subscriber turns on his mobile phone unit, it transmits a "ready to receive" signal to the nearest gateway. The signal is uplinked from the user to the satellite directly overhead. If the user is not in the same satellite footprint as the gateway,

the signal traverses ISLs until it reaches the satellite that is above the gateway. The signal is then downlinked to the gateway. If the user is not in his home gateway region, the gateway that receives the "ready to receive" signal will recognize that the user is a visiting subscriber. The gateway determines the subscriber's location and enters the information in the Visited Location Register (VLR). The visited gateway also sends information via ISLs to the subscriber's home gateway and requests both a subscriber profile and permission to set up calls for the subscriber. The home gateway sends clearance to the visited gateway and updates the user's location in the HLR.

The gateways perform call setup in the IRIDIUM® network. When a phone call is placed to an IRIDIUM® user, it is routed to the user's home gateway. This call can be placed from the PSTN or from another IRIDIUM® user. The user's home gateway determines the user location by looking up the subscriber in the HLR. The gateway then uplinks a ring signal that travels via ISL to the satellite directly above the user. The signal is downlinked to the mobile unit and it rings. When the user goes off hook, the mobile unit uplinks an off hook signal that travels via ISL to the gateway. The gateway then routes the voice packets over the IRIDIUM® network to the subscriber. Note that the voice packets do not have to be routed through the gateway. If the call is from a mobile user to a mobile user, the actual voice packets can travel completely over the IRIDIUM® ISLs. The call setup information goes through the gateway, but the gateway drops out after call setup. The scenario is slightly different if the user is in a visited gateway region. In this case, the home gateway will send a signal to the visited gateway to ring the subscriber. The visited gateway determines the user location by looking in the VLR and uplinks a ring signal that goes to the satellite over the user. When the user goes

off hook, the off hook signal is sent to the visited gateway, and then forwarded to the home gateway. Finally, the home gateway routes the voice packets via the IRIDIUM® ISLs to the satellite directly above the user. The methods used for call setup in IRIDIUM® are very similar to those used by the Advanced Mobile Phone System (AMPS) cellular telephone system [Hub97].

2.9 Network Survivability

The survivability of a telecommunications network is a measure of the network's ability to route calls or deliver messages, between any two nodes, with links or nodes removed from the network. One method of determining the survivability of a network is to represent it as a graph and determine the connectivity of the graph. Graph connectivity is a measure of either link or node redundancy in the network. Link connectivity between two nodes A and B is defined as the number of links that must be removed to disconnect A and B. Likewise, node connectivity is the number of nodes that must be removed from the network to disconnect A and B. A network in which k nodes or links must be removed in order to disconnect one or more nodes is termed k-connected. Menger's Theorem states that the maximum number of link (node) disjoint paths between nodes A and B in a connected graph is equal to the minimum number of links (nodes) that must removed to disconnect A and B [Dol93]. Applying Menger's theorem to a communications network means that the connectivity of a network is equal to the number of link or node disjoint paths. Requiring a communications network to be at least k-connected is a deterministic approach to using network connectivity as a measure of network survivability. This makes it possible to specify how many links (nodes) can fail without preventing the network from performing its function. It is also possible to use a

stochastic approach by assigning a probability of failure to individual links or nodes. This makes it possible to determine the probability that two specific nodes will become disconnected [New91, Rai91].

The ability to measure the survivability of a network by determining its connectivity leads to the concept of determining critical nodes or links. Each node and link in a network can be assigned a weight based upon how important it is to network connectivity. This is illustrated with the simple network in Figure 5. It is easy to see that nodes A and G have a node connectivity of one since all paths between these nodes go through node D. In this case, node D is a critical node in the network since its removal will disconnect nodes A and G.

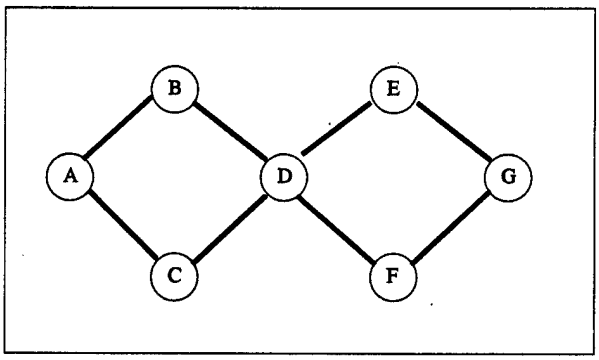

Figure 5: Simple One Connected Network

Once you are able to determine critical nodes or links, it is possible to improve the network survivability by balancing the importance of nodes or links in the network. This is accomplished by changing the physical topology of the network with the addition of nodes or links. The relative importance of the nodes for the network in Figure 5 can be balanced by adding a single link between nodes C and F. As shown in Figure 6, adding this link results in a two connected network. In order to disconnect nodes A and G, a

minimum of two nodes must be removed. The combinations of two nodes that will disconnect nodes A and G are B-C, C-D, D-F, and E-F. Note that the addition of a link between nodes B and E in Figure 5 will also produce a two-connected network. This simple example also illustrates the fact that improving the survivability of the network by adding links increases the cost of the network. It is not a trivial task to maximize the survivability and simultaneously minimize the cost of a large communications network. There are several approaches to solving this type of problem using both deterministic and stochastic computer algorithms [New91, Rai91]. The result of each of these algorithms is a balanced network in which it is difficult to determine critical nodes based upon the physical topology of the network.

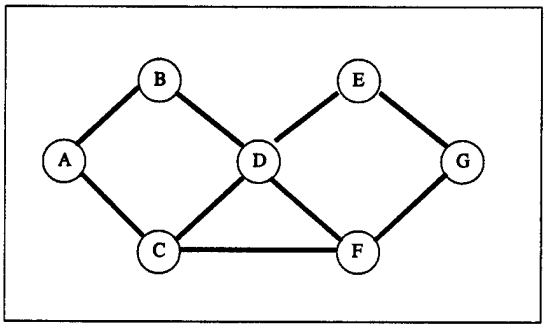

Figure 6: Simple Two Connected Network

The determination of critical nodes in a balanced network, as described above, can be accomplished if additional information about the network is available. One means of accomplishing this is to analyze the traffic flow in the network. The nodes of a network may appear equally important based upon the physical topology of the network. However, some nodes may be more important because they have a higher traffic load than other nodes. The traffic load of different nodes in the network depends upon both the routing algorithm and the distribution of traffic between transmitting and receiving

nodes. Given this information, it is possible to determine which nodes will be the most heavily loaded. In a well-connected network, the failure of a heavily loaded node may not disconnect any pair of nodes. However, the traffic that was flowing through the failed node must now be routed through other nodes. Most likely this will result in increased queuing delay in the network. It is important to note that the type of routing algorithm used will have a significant effect on the ability to determine critical nodes in this manner. A simple routing algorithm, such as the Dijkstra shortest path routing algorithm, makes no attempt to balance the load across the network. This type of algorithm is likely to produce some nodes that are much more loaded than other nodes. Likewise, a routing algorithm that attempts to balance the network load, such as the extended Bellman-Ford routing algorithm, is less likely to produce a large variance in the loading of nodes. The distribution of traffic between nodes will have a similar effect. A uniform distribution of traffic between will be less likely than a non-uniform distribution to create hot spots of highly loaded nodes. It is clear that an understanding of both the routing algorithm used and the traffic distribution is necessary to determine critical nodes in a balanced network.

2.10 IRIDIUM® Network Survivability

There is currently a lack of published research in the area of LEO satellite system network survivability. The only research currently published in open literature, in the area of IRIDIUM® network survivability, was performed by Douglas Stenger in 1996 [Ste96]. The research focused on the performance of IRIDIUM®, using three different routing algorithms, in a faulting environment. Stenger examined the performance of the Dijkstra, Extended Bellman-Ford, and Darting routing algorithms. He used IRIDIUM®

constellations with 66, 54, 42, and 30 satellites. Stenger concluded that the IRIDIUM® network performed with end-to-end delays less than 400-ms in all cases. However, long simulation times limited his research to two transmitting earth stations and a maximum loading level of 11%. While Stenger's results clearly show that the IRIDIUM® network is robust, the limited number of earth stations and low loading levels do not provide an assessment of how the network will perform under a more realistic load. In addition, Stenger did not analyze the effect that removing satellites from the constellation had on a user's ability to access the network. The removal of satellites from the constellation will cause outage times when users are unable to access the system. As the number of satellites removed increases, a user's ability to access the network decreases. At some point, the inability to access the network will become more important to the user than the delay performance. The lack of research on the survivability of LEO satellite mobile communication systems like IRIDIUM® provides the motivation for this research.

2.11 Summary

This chapter has presented an overview of the current literature in the areas of LEO satellite communications, the IRIDIUM® system, and network survivability. It began with an overview of satellite communications and a comparison of GEO, MEO and LEO satellite networks. This comparison revealed that LEO satellites have characteristics that are well suited to PCS applications. Next, the design of a LEO satellite network was examined as a tradeoff between the number of satellites required for worldwide coverage and the transmit power required in mobile units. GLOBALSTAR and IRIDIUM®, two different commercial LEO satellite networks, were compared. GLOBALSTAR utilizes a "bent pipe" approach while IRIDIUM® has both ISLs and

switching capability onboard the satellites. The establishment of ISLs and the system capacity of IRIDIUM® were explained. The call setup procedure for IRIDIUM® was explained with respect to the functions of a gateway. An overview of network survivability was presented as an introduction to a discussion of IRIDIUM® network survivability. The literature presents a large amount of information on LEO satellite networks, as well as on network survivability. Graph theory in static communication networks is well established. However, there is a lack of research in the area of mobile network survivability. This is particularly true for the area of LEO satellite networks, which serves as the motivation for this research.

CHAPTER 3

METHODOLOGY

3.1 Introduction

This chapter explains the methodology used to analyze the performance of the IRIDIUM® system and discusses the design and testing of the simulation model. Section 3.2 discusses the different methods of analysis and explains the use of simulation for this research. Section 3.3 explains how the scope of the problem was limited based on the time and computing resources available. The assumptions used in developing the simulation model are discussed in Section 3.4. Section 3.5 discusses the design of the simulation model and briefly explains its operation. The method used to scale the model and decrease the simulation run time is explained in Section 3.6. The verification and validation of the simulation model is presented in Section 3.7. The algorithm used to select critical satellites for removal is developed in Section 3.8. The simulation's input parameters are defined in Section 3.9. Finally, Section 3.10 presents the performance metrics that will be used in the analysis.

3.2 Method of Analysis

There are three possible approaches to analyzing a problem such as the performance of a communications network. These are measurement, analytical modeling, and simulation [Jai91]. Simulation is the most appropriate method of determining the IRIDIUM® network performance. Measurement of system performance requires that the system both exists and is operational. Since the IRIDIUM® system is not yet operational, measurement is easily ruled out as a method of analysis. Both the

dynamic nature and the size of the IRIDIUM® system make analytical modeling impractical. The dynamic nature of the system makes it difficult to determine the route, and thus the end-to-end delay, between two sites. The large number of nodes in the IRIDIUM® system make it difficult to analyze it as a network of queues. Computer simulation of the network is able to handle both the dynamic nature and the size of the problem. However, even simulation has limits based upon the speed of the hardware and software used. Stenger's previous research on IRIDIUM® survivability was limited due to long simulation run times [Ste96]. One of the objectives of this research is to develop a faster simulation of the IRIDIUM® network to allow simulation of high loading levels in reasonable run times.

3.3 Scope of Problem

The scope of this problem must be limited in order to model the IRIDIUM® system within the time and computing resources available. The scope of the simulation must be complex enough to provide accurate and meaningful results and at the same time limited enough to be accomplished with the resources available. There are several aspects of the IRIDIUM® system where the scope of the simulation can be limited without significantly affecting the results of an end-to-end delay analysis. These include call setup procedures, handoff procedures, numbers and types of users, and types of equipment failures.

3.3.1 Call Setup Procedures

The effect of call setup procedures will not be modeled in this research. As discussed in Chapter 2, IRIDIUM® call setup procedures use databases distributed

throughout the gateways to locate the mobile users. The focus of this study is the real time communications performance of the IRIDIUM® system. Call set up procedures add some delay in the establishment of a communications link, but do not contribute to end-to-end delay once the link is established. The call setup procedures also contribute to traffic on the network. However, it is assumed that the IRIDIUM® call setup traffic uses separate channels from actual voice or data traffic. The call setup traffic does not contribute to the end-to-end delay of network traffic by competing for network resources. Modeling the call setup procedures would significantly increase the complexity of the simulation without improving the end-to-end delay analysis.

3.3.2 Handoff Procedures

This research will account for satellite-to-satellite handoffs, but will not model beam-to-beam handoffs within a satellite footprint. The handoff of a ground station link from one satellite to another could significantly affect end-to-end packet delay. A satellite-to-satellite handoff will affect both the earth to satellite propagation delay and the shortest path to the receiving earth station. A beam-to-beam handoff will have almost no effect on either one of these delay components. Modeling each beam in the IRIDIUM® network as a queue would require 3,168 queues, while modeling only the satellites requires 66 queues. It is expected that modeling beam-to-beam handoffs will increase the runtime of the simulation without necessarily providing better end-to-end delay measurements.

3.3.3 Number and Types of Users

The IRIDIUM® users in this study will be modeled as seven stationary earth

stations and no mobile users. It is reasonable to model mobile IRIDIUM® users as a stationary earth station. As discussed in Chapter 2, the velocity of a LEO satellite is much faster than that of a mobile user in an airplane. A mobile user could leave the coverage area of one satellite and enter that of another satellite, which would cause a handoff and change the end-to-end delay. Since the satellites are traveling much faster than mobile users, satellites passing overhead will cause many more handoffs than users moving. The mobile users within a satellite footprint will generate traffic for that satellite independent of each other. It is acceptable to model this group of independent traffic sources as a single traffic source with a Poisson mean arrival rate. The location of the seven earth stations was selected so that they were distributed between 150 degrees east and 100 degrees west longitude as well as between 50 degrees north and south latitude. The intent of this was to have traffic sources and destinations evenly distributed throughout the network. The locations of the earth stations are summarized in Table 2.

Table 2: Earth Station Data

City	Longitude	Latitude	Altitude
Rio de Janeiro	-43.22	-22.90	0.01
Melbourne	144.97	-37.80	0.00
Kansas City	-94.59	39.13	0.23
Dhahran	50.00	27.00	0.76
Beijing	116.47	39.90	0.18
Berlin	13.42	52.53	0.03
Capetown	18.37	-33.93	0.00

There will also be no attempt to model traffic between mobile IRIDIUM® users and PSTN users.

3.3.4 Types of Equipment Failures

There are numerous types of equipment failures that could affect end-to-end delay

in the IRIDIUM® network. This research will focus on the complete failure of satellite communication nodes. The failure of a satellite will result in the loss of its communication links effectively removing it from the network. An actual satellite equipment failure would more likely result in reduced capability than in complete loss of communications. Complete failure of a satellite will analyze the survivability of IRIDIUM® under a worst case scenario. If the system is able to maintain acceptable end-to-end delay with the complete satellite failures, it will certainly be able to perform adequately under conditions of reduced capability.

3.4 Assumptions

The simulation model was developed using the commercial software packages SATLAB and DESIGNER by Cadence Design Systems, Inc. [Cad95]. The actual IRIDIUM® specifications were used whenever possible to create an accurate simulation. However, it was necessary to make several assumptions either when specific data on IRIDIUM® was not published in open literature, or when it was necessary to simplify the model. The rationale for these assumptions, as well as their effect on the simulation accuracy, is explained in this section.

3.4.1 Packet Size and Data Structures

The basic element that is created and transmitted through a network in DESIGNER is termed a *Data Structure*. It was therefore necessary to decide how to represent the voice traffic of the IRIDIUM® system using *Data Structures*. The simulation assumes that IRIDIUM® voice traffic can be modeled as packet voice traffic. Since the voice transmission link is already divided into TDMA slots, it was assumed that

each voice packet would be equivalent to one uplink TDMA slot. Each *Data Structure* in DESIGNER represents one voice packet. Using this assumption, the size of a voice packet can be calculated using the structure of the TDMA frame.

The size of a voice packet, representing a single time slot of the TDMA frame, is calculated to be 432 bits. The specific details of the IRIDIUM® TDMA frame, including the number of framing bits and the length of a user time slot, are not published. In addition, the type of voice encoding that will be used to provide acceptable voice quality at 4,800-bps is proprietary and is not published. However, it is not difficult to calculate the length of a TDMA time slot using the published TDMA frame length of 90-ms, the burst data rate of 50-kbps, and the sustained data rate of 4,800-bps. It is also easy to show that the known TDMA frame structure will support a sustained data rate of 4,800-bps. Each user must transmit 432 bits in a 90-ms frame to achieve a data rate of 4,800-bps.

$$4800\,bps \times 90\,ms \quad = \quad 432\,bits \tag{9}$$

A user uplink or downlink time slot with a burst data rate of 50-kbps is 8.64 ms.

$$\frac{432\,bits}{50\,kbps} \quad = \quad 8.64\,ms \tag{10}$$

The eight user time slots take up a total of 69.12-ms, which leaves 20.88-ms of the TDMA frame for framing bits and guard time slots. A possible frame structure is to use a framing time slot twice as long as an individual user time slot. This would result in 864 framing bits taking up 17.28-ms. Subtracting this value from the 20.88-ms remaining in the TDMA frame leaves 3.6-ms for guard time slots. This can be divided into eight 400-μs guard time slots between time slots in the frame, and two 200-μs guard time slots at

each end of the frame. Although the exact frame structure is not published in open literature, this approach is reasonable. It uses 4.6% of the 90-ms frame for guard time, and utilizes 76.8% of the frame for actual data bits.

3.4.2 Packet Arrival Rate

The voice packets in the model are assumed to arrive in a Poisson manner with a maximum arrival rate of 42,667 packets-per-second. Recall from Section 3.3 that each earth station represents all the users in a satellite footprint. A Poisson arrival rate was assumed because it is common to model voice communication networks with M/M/1 queues. In Section 2.7, it was shown that each satellite has a maximum of 3,840 simultaneous users. Each user is able to transmit during one uplink timeslot for each 90-ms frame. The maximum packet arrival rate is calculated using the previous assumption that each voice packet represents one uplink time slot.

$$\frac{3840\ packets}{90-ms} = 42{,}667\ packets-per-second \tag{11}$$

The minimum time between packets is 23.44-μsec.

3.4.3 Satellite Processing Delay

The satellite processing delay is assumed to be a Gaussian random variable with a mean of 14-μsec. Although it is common to model voice communications networks using M/M/1 queues, the use of an exponential service time did not seem appropriate in this situation. Since each voice packet is assumed to be the same size it is reasonable to expect the service time for each packet to be approximately equal. The use of a Gaussian random variable for satellite processing delay provides similar delays for each packet.

The selection of 14-μsec as the mean processing delay is explained as part of the loading discussion in Section 3.4.4.

3.4.4 Loading Levels

The simulation loading level represents the percent utilization of the satellite uplinks for each earth station. The simulation was run at different loading levels by varying the arrival rate for each earth station. The percent of uplink utilization, earth station arrival rates, network arrival rates, and resulting percent processor utilization are summarized in Table 3. For example, a 100% loading level means that all seven earth stations are transmitting at the maximum packet arrival rate of 42,667 packets-per-second.

Table 3: Earth Station Loading Levels

Uplink Utilization	Earth Station Arrival Rate (packets-per-sec)	Network Arrival Rate (packets-per-sec)	Processor Utilization
50%	21334	149338	30%
83%	35556	248892	50%
100%	42667	298669	60%

The network arrival rate is calculated by multiplying the earth station arrival rate by the number of earth stations. The percent utilization of the satellite switching processor in Table 3 is calculated using Equation 12 where λ is the earth station packet arrival rate and μ is the packet service rate.

$$\rho = \frac{\lambda}{\mu} \tag{12}$$

The actual processing speed of the IRIDIUM® switching processors is not published in open literature. As presented in Section 3.4.3 the mean packet processing delay, which is

the inverse of the service rate, is assumed to be 14-μsec. The assumed service rate of the switching processor should be fast enough to handle the maximum uplink traffic load plus any ISL traffic with an acceptable queuing delay. In a typical delay versus loading curve, as shown in Figure 7, the delay begins to increase exponentially at approximately 70% load. In order to keep the switching processor utilization below 70%, the processor load generated by the uplink traffic alone must be below 70%. How far below 70% this must be depends upon the amount of ISL traffic on the network. It was desired that the baseline simulation, with no satellites removed from the constellation, could accept 100% of the uplink traffic from all seven earth stations. Under this traffic load, the desired performance was defined as all end-to-end delays below 400-ms and no packet rejections.

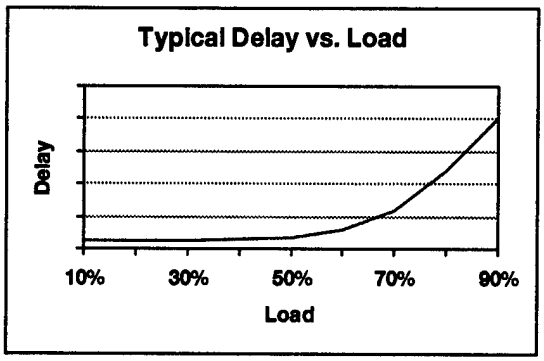

Figure 7: Typical Delay vs. Loading Curve

Pilot tests with different service rates showed that the baseline simulation performed acceptably when the maximum uplink traffic caused no more than 60% processor utilization. The service rate required to achieve this is calculated as 71,112 packets-per-second using Equation 12 where ρ equals 0.6 and λ equals 42,667 packets-per-second. The inverse of this service rate is the assumed mean satellite processing delay of 14-μsec.

3.4.5 Traffic Distribution

The simulation is run with different traffic distributions to represent different calling patterns. The traffic distribution is initially assumed to be uniform. In this case the source and destination of each packet is randomly generated with equal probability for all earth stations. In addition, the source and destination nodes of each packet are assumed to be different. This traffic distribution is summarized in Table 4.

Table 4: Uniform Traffic Distribution

Location	Transmit Probability	Destination Probability						
		Rio de Janeiro	Melbourne	Kansas City	Dhahran	Beijing	Berlin	Capetown
Rio de Janeiro	0.143	0	0.167	0.167	0.167	0.167	0.167	0.167
Melbourne	0.143	0.167	0	0.167	0.167	0.167	0.167	0.167
Kansas City	0.143	0.167	0.167	0	0.167	0.167	0.167	0.167
Dhahran	0.143	0.167	0.167	0.167	0	0.167	0.167	0.167
Beijing	0.143	0.167	0.167	0.167	0.167	0	0.167	0.167
Berlin	0.143	0.167	0.167	0.167	0.167	0.167	0	0.167
Capetown	0.143	0.167	0.167	0.167	0.167	0.167	0.167	0

An actual communications network is not likely to have a uniform traffic distribution. In this respect, the assumption of a uniform traffic distribution does not provide an accurate representation of the IRIDIUM® system. However, since the IRIDIUM® network is not yet operational there are no existing statistics on actual traffic distributions. The assumption of a uniform traffic distribution serves as a baseline in the simulation. The assumed non-uniform traffic distributions will be compared to this baseline in order to measure their effect on network performance.

The traffic distribution is next assumed to be non-uniform with a low overall network load. The non-uniform distribution is intended to simulate a high traffic load between two geographic regions of the world. These two earth stations transmit more

often than the other earth stations, and they transmit to each other more often than to the other earth stations. The remaining earth stations transmit with uniformly distributed source and destination. The two high traffic locations were selected as Kansas City and Dhahran. This non-uniform traffic distribution is summarized in Table 5.

Table 5: Non-Uniform Traffic Distribution Low Load

Location	Transmit Probability	Destination Probability						
		Rio de Janeiro	Melbourne	Kansas City	Dhahran	Beijing	Berlin	Capetown
Rio de Janeiro	0.100	0	0.167	0.167	0.167	0.167	0.167	0.167
Melbourne	0.100	0.167	0	0.167	0.167	0.167	0.167	0.167
Kansas City	0.250	0.067	0.067	0	0.667	0.067	0.067	0.067
Dhahran	0.250	0.067	0.067	0.667	0	0.067	0.067	0.067
Beijing	0.100	0.167	0.167	0.167	0.167	0	0.167	0.167
Berlin	0.100	0.167	0.167	0.167	0.167	0.167	0	0.167
Capetown	0.100	0.167	0.167	0.167	0.167	0.167	0.167	0

In order to compare this traffic distribution to the uniform case, the simulation is run with a network arrival rate of 149,338 packets-per-second. As shown in Table 3 this is the same network traffic load as that used in the 50% uplink loading level. The different transmission probabilities in the non-uniform traffic distribution result in different values for uplink loading level, earth station arrival rate, and processor utilization. These values are summarized in Table 6. It is important to note that the redistribution of traffic does not cause an uplink utilization greater than 100%.

Table 6: Non-Uniform Low Loading Levels

Transmit Probability	Uplink Utilization	Earth Station Arrival Rate (packets-per-sec)	Processor Utilization
0.25	87%	37297	52%
0.1	35%	14919	21%

The final assumed traffic distribution is a non-uniform distribution with a medium overall network load. As with the previous non-uniform distribution, Kansas City and Dhahran generate a higher percentage of the network traffic. The network arrival rate is assumed to be 248,892 packets-per-second. This is the same arrival rate as that used in the 83% uplink loading case, which allows the results to be compared with that uniform traffic distribution. This traffic distribution is shown in Table 7.

Table 7: Non-Uniform Traffic Distribution Medium Load

Location	Transmit Probability	Destination Probability						
		Rio de Janeiro	Melbourne	Kansas City	Dhahran	Beijing	Berlin	Capetown
Rio de Janeiro	0.136	0	0.167	0.167	0.167	0.167	0.167	0.167
Melbourne	0.136	0.167	0	0.167	0.167	0.167	0.167	0.167
Kansas City	0.161	0.067	0.067	0	0.667	0.067	0.067	0.067
Dhahran	0.161	0.067	0.067	0.667	0	0.067	0.067	0.067
Beijing	0.136	0.167	0.167	0.167	0.167	0	0.167	0.167
Berlin	0.136	0.167	0.167	0.167	0.167	0.167	0	0.167
Capetown	0.136	0.167	0.167	0.167	0.167	0.167	0.167	0

The uplink loading level, packet arrival rate, and processor utilization associated with these transmit probabilities is shown in Table 8.

Table 8: Non-Uniform Medium Loading Levels

Transmit Probability	Uplink Utilization	Earth Station Arrival Rate (packets-per-sec)	Processor Utilization
0.161	93%	40032	56%
0.136	79%	33815	48%

3.4.6 Routing Algorithm

The simulation assumes that packets are routed from source to destination using a "self-healing" Dijkstra routing algorithm. The algorithm calculates the shortest path from source to destination based upon the current satellite connectivity. It is a "self-healing"

algorithm because it recalculates the shortest path when the connectivity between source and destination changes. The change in connectivity could be the result of the moving satellite constellation, or the result of removing satellites from the constellation. The Dijkstra routing algorithm assumes that all nodes have instantaneous knowledge of the health and connectivity of other nodes. No attempt is made to model the overhead associated with updating the satellite routing tables. The Dijkstra algorithm calculates the shortest path based only upon cumulative propagation distance. The actual routing algorithm used in IRIDIUM® is proprietary and is not published. It is likely that the actual algorithm has the capability to balance network load by routing around heavily loaded satellites. The actual system must also have some overhead associated with updating the satellite routing tables. In this respect, the Dijkstra algorithm introduces some error into the simulation's representation of the actual IRIDIUM® system. However, the Dijkstra algorithm has the advantage that it greatly simplifies the design of the simulation model. The decision was made that the error introduced by assuming a Dijkstra routing algorithm is acceptable based upon the gains realized in simplification of the design.

3.4.7 ISL Establishment

Each IRIDIUM® satellite is capable of having up to four ISLs with adjacent satellites. A satellite can establish ISLs to the forward and aft satellites in the same orbital plane. A satellite can also establish one ISL to a satellite in each adjacent orbital plane if the horizontal pointing angle between the satellites is within the steering range of the antenna. Using a reference of zero degrees parallel to the equator, the ISL antennas are assumed to have a mean pointing angle of ± 50 degrees with a steering range of ±

22.5 degrees from the mean pointing angle. The actual steering capabilities of the IRIDIUM® ISL antennas are not published. As discussed in Chapter 2, a nominal horizontal azimuth of ± 45 to 50 degrees with an antenna steering range of 30 to 45 degrees is sufficient to maintain inter-orbital links between latitudes of 50 to 60 degrees north and south. Several pilot tests of the model were made to determine a mean pointing angle and steering range combination that performed acceptably in the model. A mean pointing angle of 50 degrees with a steering range of 45 degrees was the best combination. This combination allowed the model to establish ISLs between approximately ± 60 degrees latitude.

3.4.8 Delay Calculations

The end-to-end packet delay in this model is calculated using Equation 13.

$$T_{Packet} = T_{access} + T_{uplink} + (N-1) \cdot T_{cross} + N \cdot T_{sat} + T_{downlink} \tag{13}$$

T_{access} is the access delay associated with the multiple access technique. T_{uplink}, T_{cross}, and $T_{downlink}$ are the propagation delays for the respective links. T_{sat} is the processing and queuing delay a packet experiences at a satellite node, and N is the number of satellite nodes in the path. The effects of Doppler shift are ignored in the calculation of end-to-end packet delay.

The packet access delay, T_{access}, is assumed to be TDMA access delay with a value of 53.64-ms. The technique for calculating T_{access} for an FDMA or TDMA system is well known and the equations are widely published. The FDMA access delay is simply the packet transmission time since the FDMA channel is always available as given in Equation 14.

$$T_{FDMA} = \frac{Number\ of\ Bits\ per\ Packet}{Channel\ Transmission\ Rate\ (bps)} \tag{14}$$

The TDMA access delay depends on both the packet transmission time and the average waiting time for a TDMA slot. Under the assumption that each TDMA slot is large enough to transmit one packet, the packet transmission time is simply the TDMA slot time. The average time a user has to wait for a TDMA time slot is one half of the TDMA frame length. The TDMA access delay is described by Equation 15 where *Tf* is the TDMA frame length and *Tslot* is the TDMA slot time.

$$T_{TDMA} = \frac{Tf}{2} + Tslot \tag{15}$$

The method for calculating access delay in a system like IRIDIUM® that uses both TDMA and FDMA is not widely published. However, an analysis of the call setup procedure indicates that the IRIDIUM® access delay is simply the TDMA access delay. As discussed in Section 2.7, each cell in the IRIDIUM® system has 20 frequency channels with four TDMA users per frequency channel. When a subscriber unit goes off hook, it will receive a dial tone after a slight delay similar to that experienced with a common cordless telephone. This delay is caused by the time necessary to assign the user a frequency channel and it does not contribute to the end-to-end packet delay. It is logical to assume that the user is assigned both a frequency channel and a full duplex TDMA time slot when he receives dial tone. If a TDMA time slot is not available to assign to the user, the frequency channel could not be assigned. At this point, the user can be considered one of four users sharing a TDMA channel and the access delay can be calculated as TDMA access delay. Recall from above that the IRIDIUM® TDMA frame length is 90 ms, and the slot time is 8.64-ms. Based on the assumption that each packet is

the same length as one TDMA frame slot, the TDMA access delay is calculated 53.64-ms using Equation 15.

Propagation delay is calculated using the formula distance/speed of light. Atmospheric effects are ignored in the calculation of propagation delay. The minimum distance for an uplink or downlink is the satellite altitude of 780-km. The minimum values of T_{uplink} and $T_{downlink}$ are calculated as approximately 2.05-ms using Equation 16.

$$\frac{Distance\ to\ Satellite}{Speed\ of\ Light} = \frac{780\ km}{3x10^8\ m/s} = 2.05ms \tag{16}$$

The maximum distance for an uplink or downlink is calculated as 2,465.16-km using Equation 4 from Chapter 2. The equation is repeated here for ease of reference.

$$d = (R_e + h)\sqrt{1 + \frac{R_e}{R_e + h} - 2\frac{R_e}{R_e + h}\cos(\theta)} \tag{17}$$

The maximum values of T_{uplink} and $T_{downlink}$ are calculated as 8.22-ms using Equation 17. The values of T_{uplink} and $T_{downlink}$ calculated by the model use the actual distance between the ground station and the satellite. The propagation delay T_{cross} varies because the distance between satellites in adjacent orbits changes at different latitudes. Below latitudes of 60 degrees, where ISLs can be maintained between adjacent orbital planes, the distance between satellites varies between 3,270 and 4,480-km [Wer95]. The distance between satellites in the same orbital plane is 4,030-km [Wer95]. Using an average distance of 4,000-km between satellites results in an average T_{cross} of 13.33-ms.

$$\frac{Crosslink\ Distance}{Speed\ of\ Light} = \frac{4000\ km}{3x10^8\ m/s} = 13.33ms \tag{18}$$

The values of T_{cross} calculated by the model use the actual line-of-sight distance between the satellites.

The satellite processing and queuing delay, T_{sat}, depends on both the satellite processing delay and the loading level of the current satellite. As discussed in Section 3.4.3 the satellite processing delay is assumed to be 14-μs. The model calculates the queuing delay for each node assuming a single server First In First Out (FIFO) queue for each satellite.

3.4.9 Network Access

An earth station is assumed to have access to the satellite network when a satellite above the minimum elevation angle of 8.2 degrees is visible to the earth station. The uplink from this earth station to the satellite is assumed to be always available. No attempt is made to model the effect of local terrain or buildings on a user's ability to access the satellite. The maximum traffic load generated by an earth station, as discussed in Section 3.4.4, will not exceed the uplink capacity of a satellite. Therefore, the simulation makes no attempt to model the effects of blocking probability on a user's ability to access the network.

3.4.10 Queue Size

The maximum queue size for each satellite is assumed to be 4,000. The intent of limiting the queue size is to reject packets from the network that will clearly have an end-to-end delay in excess of 400-ms. The maximum end-to-end delay that a packet will experience is given by Equation 19 where N is the number of satellites in the path and Q is the maximum queue length.

$$T_{Max} = T_{access} + T_{uplink} + (N-1)\cdot T_{cross} + N\cdot T_{sat} + T_{downlink} + N\cdot(Q-1)\cdot T_{sat} \quad (19)$$

Pilot tests of the simulation showed that no more than seven satellites were in any path. The value of T_{Max} is plotted for different queue sizes in Figure 8. The plot assumes the maximum values of T_{access} = 53.64-ms, T_{uplink} = $T_{downlink}$ = 8.22-ms, T_{cross} = 14.93-ms, Tsat = 14-μsec and N = 7. The plot shows that the maximum end-to-end delay with a queue size of 4,000 is over 500-ms. This justifies the assumption of a maximum queue size equal to 4,000.

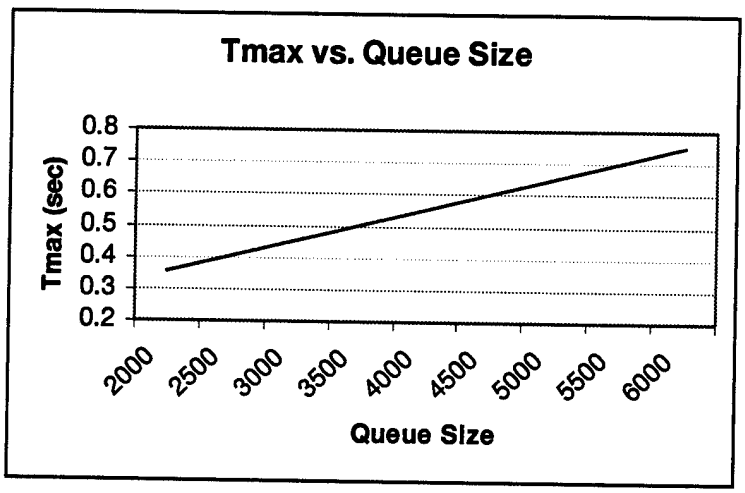

Figure 8: Maximum End-to-End Delay

3.5 Model Design

SATLAB is a satellite simulation tool that is used to design and model satellite constellations. It uses the orbital parameters of the satellites to calculate their position over a specified period of time. SATLAB also determines if satellites have line of sight visibility to other satellites and earth stations. The information calculated by SATLAB is stored in a visibility matrix, an elevation matrix, and a distance matrix. DESIGNER is a network simulation tool that is used to model and analyze communication networks. DESIGNER is able to interface with SATLAB through the BoNES SATLAB Interface

Module (BSIM). At specified intervals, DESIGNER receives the current visibility, elevation, and distance matrices from SATLAB. This information is used in DESIGNER to develop a snapshot of the IRIDIUM® system connectivity. DESIGNER is then able to treat the network as a static network for the purposes of the routing algorithm and delay calculations. Frequent updates between SATLAB and DESIGNER make it possible to use static network analysis techniques to model the dynamic aspects of the IRIDIUM® system. The combination of SATLAB and DESIGNER is well suited for the simulation of the IRIDIUM® LEO satellite network.

The top level of the simulation has two main modules, the *Positioning* module and the *Communication* module, as shown in Figure 9.

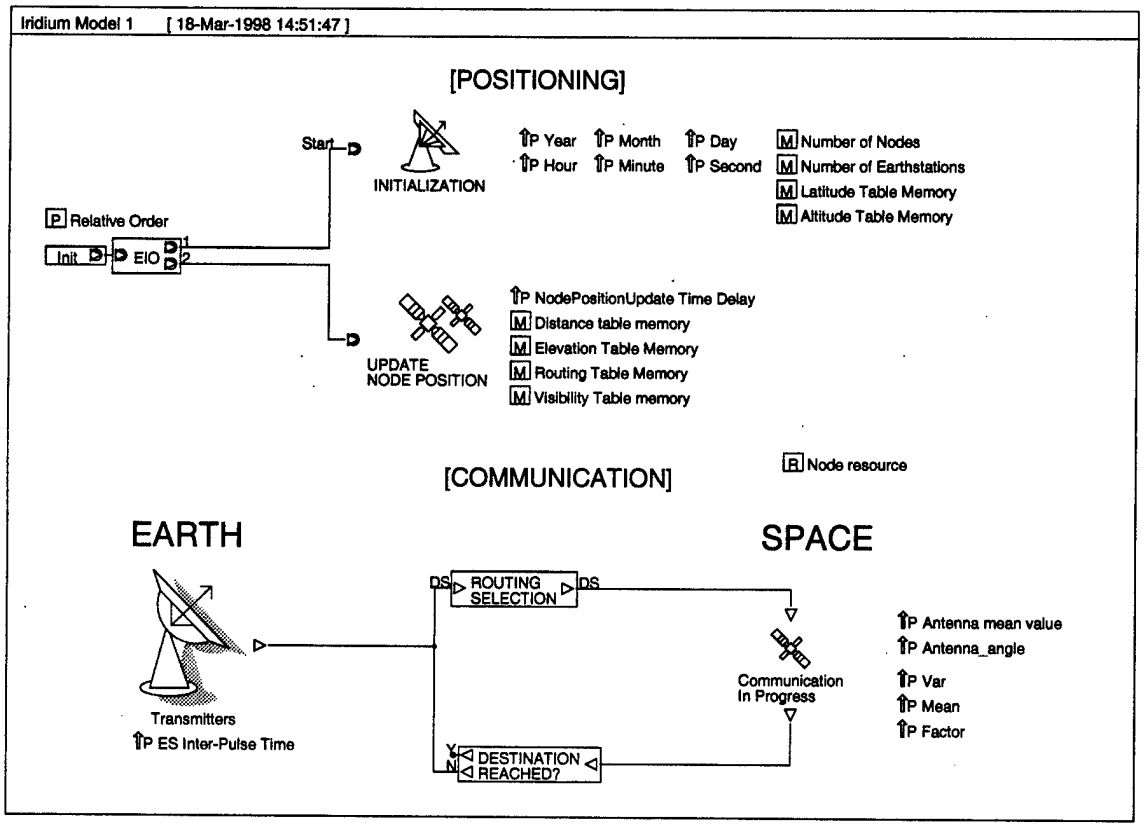

Figure 9: Simulation Top Level

The purpose of the *Positioning* module is to interface with SATLAB and develop the routing table. The module periodically updates the routing table in order to simulate the constantly changing connectivity of the IRIDIUM® network. The purpose of the *Communication* module is to generate packets, route them from source to destination, and collect information for analysis. The primary data generated for each packet is end-to-end packet delay. It is also possible to trace the path that a packet takes through the network. The *Positioning* module begins by executing the *Initialization* block. This block gets the number of earth stations from SATLAB and initializes SATLAB to the epoch start time. Next the *Update Node Position* block requests the distance, elevation, and visibility matrices from SATLAB. These values are used to develop the shortest path routing table. The *Update Node Position* block executes periodically, as specified by the Node Position Update Time Delay, and recalculates the routing table.

The *Earth Station* block generates the packets with a Poisson arrival rate. For the purposes of the simulation, the packet is actually a data structure with fields summarized in Table 9. The Sequence Number is a counter that sequentially numbers the packets. The Source, Destination, Current Node, and Next Node fields are used to determine the route and to determine if the packet has reached its destination. The Current Node or Next Node fields can also be used to trace a packet's path through the network. TNOW is the simulation run time in seconds. The Delay field is incremented by various modules as the packet traverses the network and it measures end-to-end packet delay. The Hop Count field is incremented at each node in the path from Source to Destination. Once the packet is generated, it is passed to the *Routing Selection* block.

Table 9: Data Structure Fields

Field Name	Type	Description
Sequence Number	Integer	Sequentially number packets
Source	Integer	Node sending packet
Destination	Integer	Destination of packet
Current Node	Integer	Current location of packet
Next Node	Integer	Next node in path to destination
TNOW	Real	Simulation run time
Delay	Real	Cumulative end to end delay
Hop Count	Integer	Cumulative number of nodes in path

The *Routing Selection* block reads the Current Node and Destination fields. It then accesses the routing table to determine the next node in the path. The block updates the Next Node field, increments the Hop Count field, and passes the packet to the Space block.

The *Space* block determines if the next link is satellite-to-satellite, earth-to-satellite, or satellite-to-earth based upon the Current Node and Next Node fields. A different block is used to calculate the delay for each type of link. The delay for both a satellite-to-satellite link and a satellite to earth link are calculated based upon propagation delay, and the satellite processing and queuing delay. The delay for an earth-to-satellite link is calculated using an earth station processing delay, TDMA access delay, and propagation delay. The Space block receives the delay calculation from the appropriate block and updates the Delay field in the packet. It then passes the packet to the *Destination Reached* block.

The *Destination Reached* block reads the Next Node and Destination fields to determine if the packet has reached its destination. If the fields are the same, the packet has reached its destination and it stops traversing the network. If they are not the same, the Next Node field is written to the Current Node field. The packet is then passed to the *Routing Selection* block. The packet will continue to cycle through the *Routing*

Selection, *Space*, and *Destination Reached* blocks until the Destination and Current Node fields match.

3.6 Simulation Scaling

A simulation in DESIGNER that attempts to model the actual traffic load of the IRIDIUM® network will run very slowly. Stenger's previous analysis of the IRIDIUM® network was limited by long simulation times to two earth stations transmitting at an 11% uplink loading level. Even at this low loading level, the simulation ran for two to three weeks to simulate fifteen minutes of real time. One of the goals of this research is to evaluate the IRIDIUM ® system at high loading levels. This can only be accomplished with the computing resources available by improving the simulation speed.

Several pilot tests of the simulation were conducted to determine which parameters had the greatest effect on run time. First, the simulation was run with a low loading level and the node update time was varied from 1-s to 180-s. Since the simulation must pass data from SATLAB to DESIGNER at each node update time, it was expected that this parameter would effect the run time. These pilot tests revealed that simulations with a node update time above 20-seconds ran at approximately the same speed. The node update time did not significantly increase the simulation runtime unless it was below 20-seconds. Next, the simulation was run with a fixed node update time of 30-seconds and varying loading levels. This revealed that the simulation run time increased in direct proportion to the number of packet-per-second generated in the model. Based on this, the decision was made to scale the simulation to model a percentage of the actual traffic load.

Modeling a percentage of the actual traffic load must be accomplished in a manner that does not change the simulation's calculation of end-to-end delay. All aspects of the simulation used to calculate delay must be scaled by the same factor. Dividing the arrival rate λ by a factor F scales the traffic load. Since the packet inter-arrival time is the inverse of λ, scaling the arrival rate effectively multiplies the inter-arrival time by F. In order to apply the scaling factor to all aspects of the model all times in the model must be multiplied by the same factor F. The times that contribute to the end-to-end delay are processing delay, propagation delay, and queuing delay. The processing delay, which is the inverse of the service rate μ, is an input parameter to the simulation. This time is easily multiplied by the scaling factor F. The propagation delay of each link is also multiplied by the scaling factor. The simulation calculates the queuing delay at each node. The average service time T_{av}, which includes both queuing delay and processing delay, is given by Equation 20.

$$T_{av} = \frac{1}{\mu - \lambda} \tag{20}$$

The average queuing delay W is obtained by subtracting the average processing delay from T_{av}. This is shown in Equation 21.

$$W = \frac{1}{\mu - \lambda} - \frac{1}{\mu} \tag{21}$$

Note that both μ and λ have already been scaled by a factor of $1/F$. Therefore the queuing delay W calculated by the simulation will already be multiplied by the scaling factor F. The cumulative end-to-end delay calculated for each packet in the simulation will be the actual delay multiplied by the scaling factor F. In order to analyze this delay

in terms of real time communication constraints, it must be converted back into real time. This is accomplished by dividing the delay field of each packet by the scaling factor when the packet reaches its destination.

Several pilot tests of the simulation were conducted to determine the effect of the scaling factor. First, the simulation was run both scaled by a factor of 1,000 and non-scaled to ensure that the scaling factor did not change the output of the model. This pilot test was conducted with two earth stations for 60 seconds of simulation time. The average end-to-end delay of all packets in the scaled test was 120.87-ms with a standard deviation of 3.32-ms. The non-scaled test produced an average delay of 120.86-ms with a standard deviation of 0.3-ms. The lower standard deviation in the non-scaled test can be explained by the fact that approximately 1,000 times as many packets were generated. Next, the simulation was run with different scaling factors to determine a suitable value of F. These pilot tests were conducted with all seven earth stations transmitting at a 100% link load. With a scaling factor of 10,000, the simulation ran for approximately two hours to simulate 40 minutes of real time. Recall that Stenger's previous model ran for over two weeks to simulate two earth stations transmitting at an 11% link load for 15 minutes of real time. The simulation scaling results in a significant improvement in the simulation run time that will allow the system to be evaluated at high loading levels.

3.7 Model Verification and Validation

The simulation was tested thoroughly to ensure that it accurately modeled the IRIDIUM® network. The model verification included tests to ensure that the model design was sound. The model validation consisted of tests to determine if the outputs of the model provided an accurate representation of the IRIDIUM® system.

3.7.1 Verification

The verification of the model was performed at two levels. First, the individual blocks used in the model were tested to ensure that they were performing as expected. Then the entire model was tested to determine if the complete model was functioning properly. In addition to these two levels of testing, DESIGNER has built in functions that check for errors each time a block is saved in the model. These functions ensure that input and output parameters of blocks are assigned with the correct variable types. They also check for missing connections between blocks in a module. DESIGNER will not allow a simulation to be run if it does not pass these checks.

The verification of the individual blocks revealed that the *TDMA Access Delay* block provided with SATLAB was not functioning as expected. Increasing the packet arrival rate resulted in an exponentially increasing access delay. As a result, access delay could become the major delay factor in end-to-end packet delay. An examination of the C code used in the *TDMA Access Delay* block showed that the formulas used to calculate access delay assumed an infinite user population. In the actual IRIDIUM® system the number of users is limited based on the TDMA frame structure and the number of frequency channels available. If all of the available frequency channels and their associated TDMA time slots are in use then additional users will be blocked from the system. Additional attempts to access the system, above the system capacity, will not contribute to the packet access delay for those users already assigned frequency and time slots. For this reason, the *TDMA Access Delay* block was replaced with a fixed delay time of 53.64-ms as discussed in Section 3.4.8.

The verification of the entire model consisted of varying the inputs to the model and determining if they had the expected effect on model outputs. In addition to model outputs, the path that a packet took through the network was examined. The effect of changing inputs was tested to determine if the logic of the entire model was sound. The path was examined to ensure that the routing algorithm was functioning properly and that the *Communication* module was receiving accurate information from the *Positioning* module.

The test of the model inputs and outputs demonstrated that the logic of the model was sound. The inputs tested were packet arrival rate, traffic distribution, and satellite removal. The test of packet arrival rate measured the number of packets generated in the simulation to ensure that the traffic generator was performing correctly. It also measured the average end-to-end delay to ensure that it increased with heavier loads as expected. The test of the traffic distribution counted the number of packets transmitted and received at each earth station for each traffic distribution. The results were compared to the uniform and non-uniform traffic distribution tables in Section 3.4.5 to ensure proper operation. The test of satellite removal began by determining the path that a packet took between two cities. Then one satellite in the path was removed by setting its altitude to a negative number. The simulation was run again to ensure that the packets no longer used the removed satellite in its path. All of these tests gave the expected results demonstrating that the logic of the model is sound.

The test of the route that a packet took through the network revealed that the *Satcom Router* block in SATLAB was not generating a routing table that accurately modeled the IRIDIUM® system. The routing table took into account line-of-sight

visibility between satellites, but allowed packets to be routed between nonadjacent orbital planes. For example, a packet could go from a satellite in orbital plane one to a satellite in orbital plane three. This problem was brought to the attention of two of the developers of SATLAB, and they provided C code for a new routing block that accurately modeled the inter-orbit IRIDIUM® links. They had developed this code for research they were performing in the area of antenna pointing angles for LEO satellites [Kel96]. This code was implemented in a Designer primitive block, and the new routing block performed as expected.

3.7.2 Validation

The validation of the model consisted of comparing the end-to-end delay values generated by the model with theoretical values. The theoretical values were calculated using the equations in Section 3.4.8. Since the IRIDIUM® network is not yet operational it is impossible to compare the model outputs with actual measured data. However, the order of magnitude of the delay can be compared to real time communication requirement of 400-ms. Pilot tests of the simulation were conducted with a low loading level and a full satellite constellation. The low load was used to minimize the effects of queuing delay since this is difficult to calculate using the equations in Section 3.4.8. The number of satellites in the path was determined using the Hop Count field of the received packet. The delay values output by the simulation were consistent with the calculated values in all cases.

3.8 Algorithmic Selection of Failed Satellites

The intent of analyzing the IRIDIUM® system performance with a degraded satellite constellation is to determine how many satellites can fail before the network performance becomes unacceptable. Therefore, it is desirable to determine which satellites are most important with regard to network end-to-end delay. Before developing an algorithm to determine the critical satellites, it is necessary to examine how failed satellites affect end-to-end delay. This makes it possible to define the scope of the algorithm.

The effect of a failed satellite on end-to-end delay varies over time for each earth station. At some times the satellite is not in the path from the earth station to any other earth station. At these times the failure of the satellite has no effect on the end-to-end delay of packets transmitted from the earth station. The satellite is in the shortest path to other earth stations during some time periods. The loss of the satellite at these times will increase the end-to-end delay to other earth stations because the packets must take alternate longer paths. Finally, the satellite may provide the only uplink for the earth station for a certain period of time. During this time, the loss of the satellite will prevent the earth station from transmitting. It is clear from this discussion that a satellite's failure effects geographically separated earth stations differently at any given time.

The preceding discussion suggests that the effect of failed satellites on end-to-end delay should be analyzed for a single transmitting earth station and for a limited period of time. It also illustrates that the removed satellites must not disconnect the earth stations in order for packets to travel between them. Therefore, the decision was made to have the algorithm find the critical satellites for packets leaving Kansas City during a ten-

minute period while the uplink satellite remained the same. The algorithm would also be prevented from removing the uplink satellite or any other satellite that disconnected the network. With the scope of the algorithm defined, it is now necessary to determine how the algorithm will select critical satellites.

The selection of critical nodes, as discussed in Section 2.9, can be based either on the network topology or on the loading of the nodes. Because each satellite has up to four ISLs, it is not possible to select critical satellites based only upon the network topology. So, the algorithm to select critical satellites should be based on the satellite loading level. One measure of a satellite's loading is the number of paths it is in. For example, the path that packets take from Kansas City to all other earth stations can be determined. The removal of the node that is in the greatest number of paths will affect the end-to-end delay to more earth stations than any other node. As such, this satellite is the most critical node. Pilot tests were conducted to test the effect of removing these satellites on end-to-end delay. The tests indicated that up to seven satellites would need to be removed at low loading levels to significantly impact end-to-end delay. This led to the decision to have the algorithm remove three, five and seven satellites.

The discussion in this section provides the basis for the development of the following algorithm. This algorithm is used to select the critical satellites that are removed from the constellation:

1. Generate packets and determine the paths from Kansas City to all others.
2. Count the number of paths that each satellite is in.
3. Remove the satellite in the most number of paths that does not disconnect the network. In the case of a tie, remove the satellite closest to Kansas City.

4. Remove the satellite in the second most number of paths that does not disconnect the network and is not in the same path as the satellite removed in step 3. In the case of a tie, remove the satellite closest to Kansas City.
5. Remove the satellite in the third most number of paths that does not disconnect the network and is not in the same path as the satellites removed in steps 3 or 4. In the case of a tie, remove the satellite closest to Kansas City.
6. Repeat steps 1 through 4 to select the fourth and fifth satellites.
7. Repeat steps 1 through 4 to select the sixth and seventh satellites.

3.9 Input Parameters

The input parameters of the simulation are the parameters that are changed to create different test cases. Each of these parameters has been previously mentioned in this chapter. They are defined below with the range of values that will be used.

3.9.1 Loading Level

The loading level is defined as the percent utilization of the earth station uplinks. This parameter is adjusted by changing the mean time between packet arrivals. The values that will be used for loading level are 50%, 83% and 100%, as discussed in Section 3.4.4.

3.9.2 Number of Satellites Removed

This parameter is the defined as the number of failed satellites in the constellation. The failed satellites will be selected using the algorithm discussed in Section 3.8. The values that will be used for number of satellites removed are 3, 5 and 7.

3.9.3 Traffic Distribution

The traffic distribution is defined as the probability that a packet is transmitted between each pair of nodes. The traffic distributions will be made according to the tables presented in Section 3.4.5. These tables correspond to a uniform distribution, a non-uniform distribution at low load, and a non-uniform distribution at medium load.

3.10 Performance Metrics

3.10.1 End-to-End Delay

The end-to-end packet delay is defined as the mean packet delay for packets transmitted from Kansas City to all other earth stations. The model calculates the delay for each packet using the equations in Section 3.4.8. This is the primary measure of network performance. The benchmark for end-to-end packet delay is 400-ms, and a delay higher than this indicates unacceptable performance.

3.10.2 Packet Rejection Rate

The packet rejection rate is defined as the ratio of rejected packets to transmitted packets. Rejected packets are defined as the number of packets that leave the sending earth station but do not reach the receiving earth station due to the overflow of queues in the network model. The benchmark for packet rejection rate is 1%, and a rejection rate higher than this indicates unacceptable performance.

3.10.3 Average Number of Visible Satellites

The average number of visible satellites is defined as the mean number of satellites visible from a given earth station over a 24-hour period. The mean number of

satellites is calculated using Equation 22 where n is the number of satellites visible, and $p(n)$ is the percentage of 24-hours that n satellites are visible.

$$\overline{E}(n) = \sum_{x=0}^{n} p(n)n \tag{22}$$

The benchmark for average number of visible satellites is 1.44, which is the mean value for all scenarios tested.

3.10.4 Cumulative Outage Time

Cumulative Outage Time is defined as the total number of minutes that an earth station is unable to access the network in a 24-hour period. The ability to access the network is defined in Section 3.4.9. The IRIDIUM® system is designed so that a user anywhere in the world will have continuous access to the network through at least one of the 66 satellites. As a result of the non-operational satellites in this research, there will be times during a 24-hour period when a user will have no satellite available to access the network. This is very different from a traditional terrestrial network due to the dynamic nature of the IRIDIUM® network. In the IRIDIUM® network, a non-operational satellite node will pass overhead and within approximately ten minutes the user will have network access through another satellite. In a terrestrial based network, a non-operational node will deny local users access to the network for the entire 24-hour period. The benchmark for Cumulative Outage Time is 55.41-minutes, which is the mean value for all scenarios tested.

3.10.5 Maximum Continuous Outage Time

Maximum Continuous Outage Time is defined as the maximum continuous time that an earth station is unable to access the network in a 24-hour period. The ability to access the network is defined in Section 3.4.9. As discussed in Section 3.10.4, the dynamic nature of the IRIDIUM® system makes it very different than a traditional terrestrial system when nodes become non-operational. In a terrestrial network, the failure of a node will result in a continuous outage time of 24-hours for local users. In the IRIDIUM® network, the failure of several satellite nodes will result in a continuous outage time less than 30-minutes. The benchmark for Maximum Continuous Outage Time is 12.04-minutes, which is the average value of all scenarios tested.

3.11 Summary

This chapter has presented the methodology used to develop the simulation model. The development of a simulation model required that the scope of the problem be limited. The model design and the facts and assumptions used in the model were explained. Both the method of scaling the model and the algorithm for selecting critical satellites were developed. The process used to validate correct operation of the simulation model was explained. Finally, the input parameters and measured outputs of the model were defined and explained.

CHAPTER 4

ANALYSIS

4.1 Introduction

The purpose of this chapter is to present an analysis of the data generated with the simulation. The chapter begins with a discussion of the statistical accuracy of the data in Section 4.2. The analysis of the IRIDIUM® system was conducted in two parts. First, it was assumed that the user could access the network despite the non-operational satellites. Using this assumption, an analysis was made of both the end-to-end delay and the packet rejection rates from Kansas City to all other earth stations. This is covered in Sections 4.3 through 4.5. Section 4.3 defines the test scenarios that were used. In Section 4.4, an analysis of the end-to-end delay and packet rejection for all test scenarios is presented. An analysis of each test scenario is presented in Section 4.5. The second part of the analysis focuses on an earth station's ability to access the network as satellites fail. This is presented in Sections 4.6 through 4.8. In Section 4.6, the network access scenarios are defined. An analysis of the average number of visible satellites, cumulative outage time, and maximum outage time for all scenarios is presented in Section 4.7. Section 4.8 provides an analysis of each network access test scenario. Finally an overall assessment of the IRIDIUM® system combining both approaches is made in Section 4.9.

4.2 Statistical Accuracy

The simulation was run with different random number generator seed values to ensure that the end-to-end delay results were independent of a specific Poisson traffic arrival pattern. Three different seed values were used for each combination of input

parameters tested. This produced three sample means of the end-to-end delay between Kansas City and each other earth station. The 95% confidence interval of the mean end-to-end delay was calculated using the *student's t-distribution* as shown in Equation 23 where $\bar{x}$ is the average sample mean, s is the standard deviation of the sample means, n is the number of sample means, and t is the *student's t-distribution* [Jai91].

$$100(1-\alpha)\%\,CI \quad = \quad \bar{x} \pm t\,[1-\alpha; n-1]\,s/\sqrt{n} \tag{23}$$

There is an inherent variance in the end-to-end delay between two earth stations in the IRIDIUM® network. This variance is the result of the dynamically changing path, and corresponding changing propagation distance, between two earth stations as the satellite constellation moves. Based upon this inherent variance, a confidence interval of 95% was selected to express the statistical accuracy of the data. A 95% confidence interval provides high confidence that the variance in end-to-end delay is within a range that is orders of magnitude less than the mean end-to-end delay value. The 95% confidence interval for the end-to-end delay from Kansas City to other earth stations with a uniform traffic distribution and low loading level is shown in Table 10. The 95% confidence interval for the mean end-to-end delay is less than ±1.5-ms for each earth station in Table 10. This shows that three runs of the simulation with different seed values are sufficient to produce a small confidence interval using the given input test parameters. It is expected that the variance in end-to-end delay will be greater at high loading levels with several non-operational satellites. The 95% confidence interval for the end-to-end delay from Kansas City to all other earth stations with a non-uniform traffic distribution, medium loading level, and seven non-operational satellites is shown in Table 11.

Table 10: 95% CI for Uniform-Low-Load With a Full Satellite Constellation

From Kansas City to:	Average Sample Mean	Standard Deviation	95% Confidence Interval	
			Minimum	Maximum
Dhahran	0.12600	0.00005	0.12588	0.12613
Melbourne	0.13721	0.00024	0.13660	0.13781
Beijing	0.11384	0.00046	0.11268	0.11499
Capetown	0.12842	0.00049	0.12721	0.12964
Rio	0.09817	0.00035	0.09730	0.09904
Berlin	0.12377	0.00015	0.12340	0.12415

Table 11: 95% CI for Non-uniform-Medium-Load and Seven Non-operational Satellites

From Kansas City to:	Average Sample Mean	Standard Deviation	95% Confidence Interval	
			Minimum	Maximum
Dhahran	0.29957	0.00384	0.29002	0.30911
Melbourne	0.22685	0.00391	0.21715	0.23656
Beijing	0.28026	0.00309	0.27259	0.28794
Capetown	0.29050	0.00718	0.27267	0.30834
Rio	0.26172	0.00202	0.25671	0.26673
Berlin	0.21488	0.00048	0.21368	0.21608

The 95% confidence interval is less than ± 17-ms for each earth station in Table 11. This shows that even under conditions with a high variance in mean end-to-end delay, three runs of the simulation with independent seed values are sufficient. From this point on, the values shown for mean end-to-end delay represent the average mean end-to-end delay as depicted in Table 10 and Table 11. Similar tables with the confidence intervals for all simulation runs are given in the Appendix.

4.3 Delay Test Scenarios

The analysis of end-to-end delay and packet rejection rate was conducted using five different test scenarios. The scenarios represent a combination of the simulation's input parameters *Loading Level* and *Traffic Distribution* as defined in Sections 3.9.1 and

3.9.3 respectively. Each of the test scenarios was run with zero, three, five, and seven non-operational satellites. The non-operational satellites were selected according to the algorithm presented in Section 3.8.

4.3.1 Uniform Distribution Low Load

This scenario serves as a baseline for comparison with the other defined scenarios. It represents the network operating with little strain from either the traffic distribution or the loading level. It uses the uniform traffic distribution presented in Table 4. Each of the seven earth stations has an uplink utilization level of 50%. As shown in Table 3, this corresponds to a network arrival rate of 149,338 packets-per-second with each of the seven earth stations generating 21,334 packets-per-second. Since this scenario uses a low loading level, there should not be a significant amount of queuing delay with a full satellite constellation.

4.3.2 Uniform Distribution Medium Load

This scenario models the network under a moderate offered load. As in the previous scenario, it uses the uniform traffic distribution presented in Table 4. The uplink utilization level is increased to 83% for each of the seven earth stations. As shown in Table 3, this represents a network arrival rate of 248,892 packets-per-second with each earth station generating 35,556 packets-per-second. It is expected that the end-to-end delay with a full satellite constellation will increase from the previous scenario due to the effects of queuing delay.

4.3.3 Uniform Distribution High Load

This scenario models the network with a high loading level. The scenario uses

the uniform traffic distribution presented in Table 4. Each of the earth stations transmits at a maximum uplink utilization level of 100%. As shown in Table 3, this represents a network arrival rate of 298,669 packets-per-second with each earth station generating 42,667 packets-per-second. It is expected that queuing delay will have a significant impact on the end-to-end delay in this scenario.

4.3.4 Non-uniform Distribution Low Load

This scenario models the network with two earth stations transmitting and receiving most of the traffic and a low network offered load. It uses the non-uniform traffic distribution presented in Table 5. As discussed in Section 3.4.5, an actual network is not likely to have a uniform traffic distribution. This scenario will analyze the effect of a more realistic traffic distribution on network performance. The network arrival rate is 149,338 packets-per-second, which is the same as that used in the *Uniform Low Load* scenario described in Section 4.3.1. Since the traffic is not uniformly distributed between the earth stations, they do not all transmit at an uplink utilization level of 50%. Kansas City and Dhahran transmit at approximately 88% uplink utilization, while the remaining earth stations transmit at approximately 35% uplink utilization.

4.3.5 Non-Uniform Distribution Medium Load

This scenario models the network with two earth stations transmitting and receiving most of the traffic and a moderate network offered load. It uses the non-uniform traffic distribution presented in Table 7. As discussed in Section 3.4.5, an actual network is not likely to have a uniform traffic distribution. This scenario will analyze the effect of a more realistic traffic distribution on network performance. The network

arrival rate is 248,892 packets-per-second, which is the same as that used in the *Uniform Medium Load* scenario described in Section 4.3.2. Since the traffic is not uniformly distributed between the earth stations, they do not all transmit at an uplink utilization level of 83%. Kansas City and Dhahran transmit at approximately 94% uplink utilization, while the remaining earth stations transmit at approximately 79% uplink utilization.

4.4 Analysis of Delay Performance Metrics

The primary measurements used to assess the IRIDIUM® network's ability to provide real-time communications were the mean end-to-end packet delay and the packet rejection rate as defined in Sections 3.10.1 and 3.10.2. The simulation was designed to operate with both an end-to-end delay less than 400-ms and a packet rejection rate less than 1% using the *Uniform High Load* input parameters described in Section 4.3.3 and a full satellite constellation. Both the maximum end-to-end delay and the packet rejection rate are dependent upon the maximum queue size defined in Section 3.4.10. Increasing the queue size will reduce the packet rejection rate at the expense of increased end-to-end delay. Likewise, decreasing the queue size will reduce the end-to-end delay at the expense of increased packet rejections. Both of these parameters must be taken into consideration when assessing the network performance.

4.4.1 Delay Analysis

The mean end-to-end packet delay measured from Kansas City to all other earth stations was below 400-ms for all test scenarios. The lowest mean end-to-end delay was 98.17-ms between Kansas City and Rio de Janeiro in the *Uniform Low Load* scenario

with a full satellite constellation. The highest mean end-to-end delay was 290.021-ms between Kansas City and Dhahran in the *Non-uniform Medium Load* scenario with seven non-operational satellites. The fact that no scenarios had a mean end-to-end packet delay above 400-ms was expected based upon the selection of queue sizes presented in 3.4.10. The queue size was selected so those individual packets with an end-to-end delay in excess of 400-ms would be rejected from the network. A detailed examination of the data showed that a small number of packets took approximately 380-ms to 390-ms to reach their destination. With only a small number of packets approaching 400-ms end-to-end delay, an average end-to-end delay of 290-ms is reasonable.

The end-to-end delay performance had several trends that illustrated the effect of varying the different input parameters. The first was that increasing the loading level for a given traffic distribution with a full satellite constellation had a significant impact on queuing delay. This is illustrated for a uniform traffic distribution with a full satellite constellation in Figure 10.

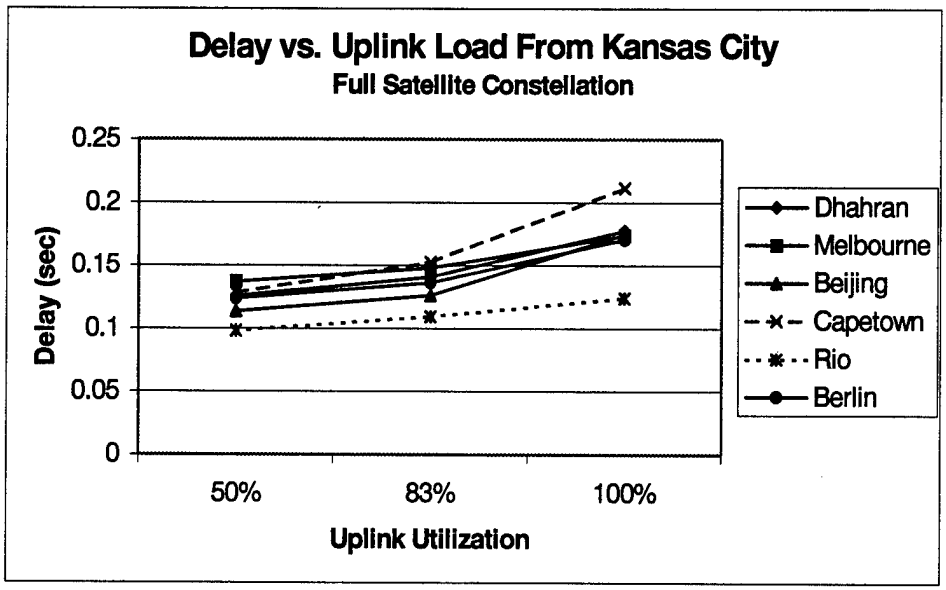

Figure 10: Delay for Uniform Distribution and Full Constellation

For most of the cities in Figure 10, there was a much larger increase in end-to-end delay when the uplink utilization was increased form 83% to 100% then when it was increased from 50% to 83%. This indicates that the effects of queuing delay with a full satellite constellation are most significant above 83% uplink utilization.

The second trend was that non-operational satellites had a significant impact on both queuing delay and end-to-end delay. Figure 11 plots the same uniform traffic distribution and uplink utilization as Figure 10, but has seven non-operational satellites.

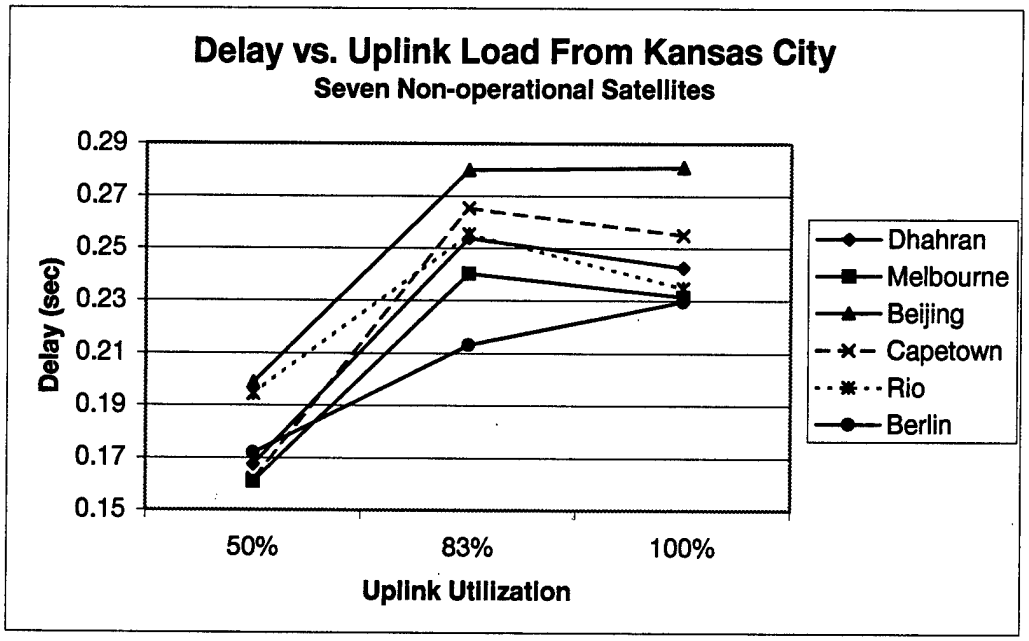

Figure 11: Delay for Uniform Distribution and Seven Non--operational Satellites

Most of the cities in Figure 11 experienced a significant increase in end-to-end delay when the uplink loading is increased from 50% to 83%. The delay either leveled off or decreased when the utilization was increased from 83% to 100%. This indicates that the seven non-operational satellites significantly increased the queuing delay in the network between the low loading level of 50% uplink utilization and the moderate level of 83% uplink utilization. The leveling off or decrease between the 83% and 100% uplink

utilization levels was a result of increased packet rejections. Those packets with end-to-end delays above 400-ms were rejected which resulted in a decrease of the mean end-to-end delay of all packets successfully transmitted between the cities.

A third trend was that the non-uniform traffic scenarios had higher end-to-end delay than the uniform traffic scenarios with the same network arrival rate. The traffic distributions used in the *Non-uniform Low Load* and the *Non-uniform Medium Load* scenarios both had a high traffic link between Kansas City and Dhahran. As discussed in Section 4.3.4, the *Non-uniform Low Load* and *Uniform Low Load* scenarios had the same network arrival rate. Similarly, the *Non-uniform Medium Load* and *Uniform Medium Load* scenarios used the same network arrival rate. The end-to-end delay between Kansas City and Dhahran is plotted against the number of non-operational satellites for each of the test scenarios in Figure 12.

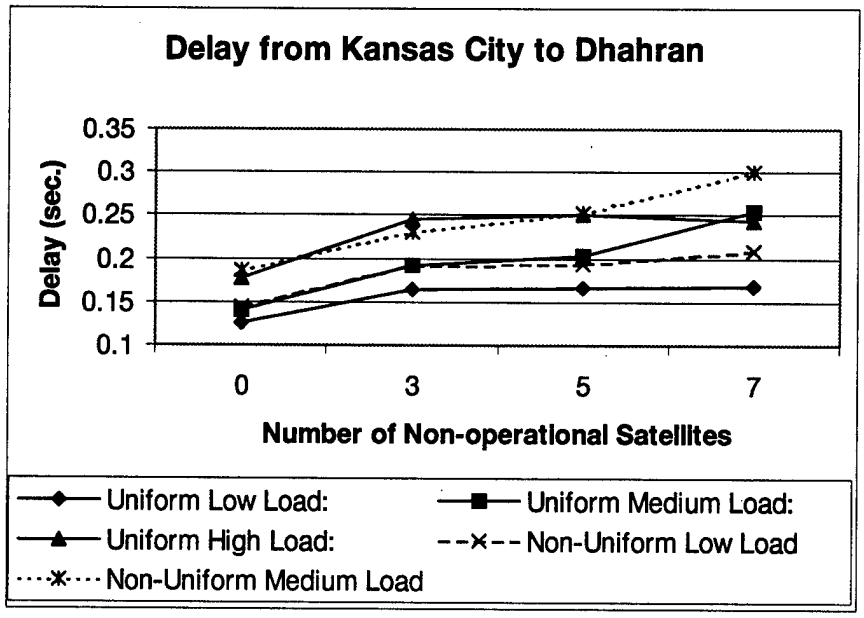

Figure 12: Delay from Kansas City to Dhahran

Figure 12 illustrates that the non-uniform traffic distribution increased the end-to-end delay at both the low and medium loading levels. The *Non-uniform Low Load* scenario

had a higher end-to-end delay than the *Uniform Low Load* scenario, while the *Non-uniform Medium Load* scenario had a higher end-to-end delay than the *Uniform Medium Load* scenario. This result held true not only for the high traffic link of Kansas City to Dhahran, but for other earth stations as well. The end-to-end delay between Kansas City and Berlin is plotted against the number of non-operational satellites for all scenarios in Figure 13.

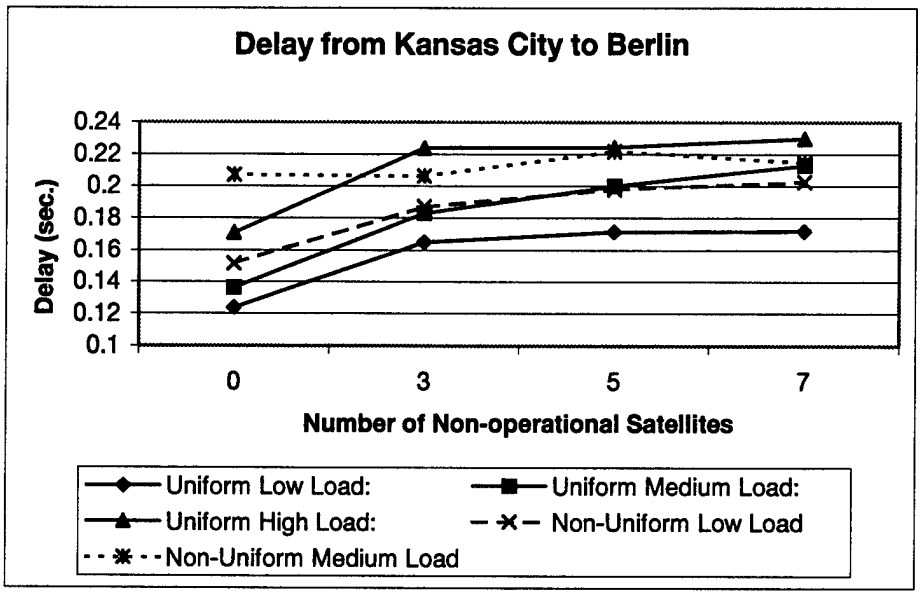

Figure 13: Delay from Kansas City to Berlin

Figure 13 illustrates that the non-uniform traffic distribution had the same effect on end-to-end delay from Kansas City to Berlin that it had on that from Kansas City to Dhahran. The *Non-uniform Low Load* scenario had a higher end-to-end delay than the *Uniform Low Load* scenario, while the *Non-uniform Medium Load* scenario had a higher end-to-end delay than the *Uniform Medium Load* scenario.

4.4.2 Packet Rejection Analysis

The packet rejection rate varied between 0% and 8.98% across all of the test

scenarios. The low load scenarios had the best performance with respect to packet rejection. Both the *Uniform Low Load* and the *Non-uniform Low Load* scenarios had no packet rejections with up to seven non-operational satellites. The *Non-uniform Medium Load* scenario had the worst packet rejection rate of 8.98% and was also the only scenario that rejected packets with a full satellite constellation. The packet rejection rate is plotted against the number of non-operational satellites for all scenarios in Figure 14.

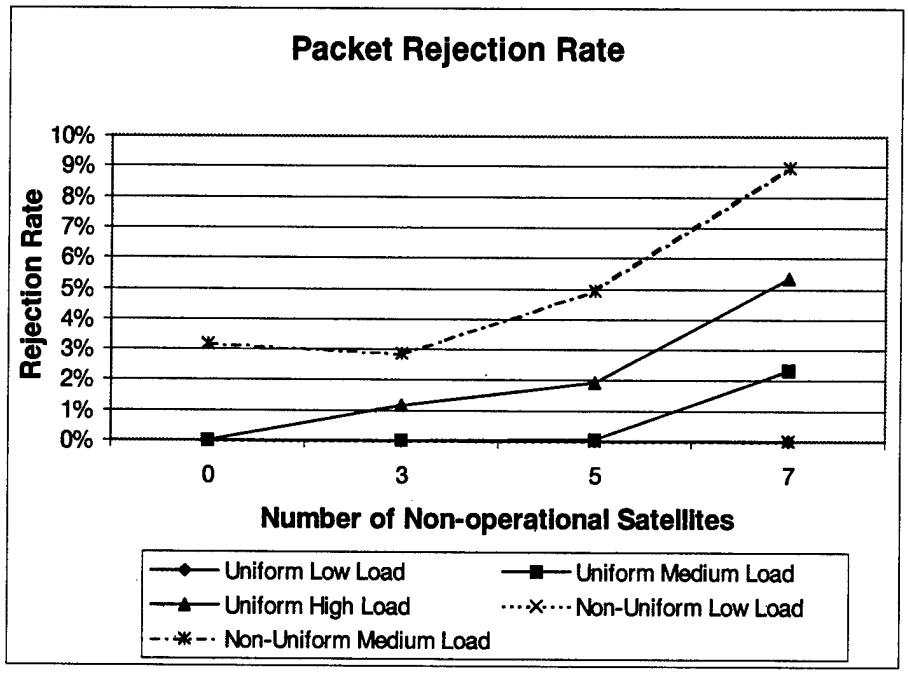

Figure 14: Packet Rejection Rate for Each Scenario

Figure 14 illustrates that the packet rejection rate increased with both the loading level and the number of non-operational satellites. Since the end-to-end delay was below the benchmark of 400-ms for all scenarios, the packet rejection rate was the performance metric that determined acceptable performance. The benchmark for packet rejection was defined as 1% in Section 3.10.2. Figure 14 shows several trends in the packet rejection rate. First, with a full satellite constellation, the distribution of traffic had a more significant impact on network performance than the loading level. The *Non-uniform*

Medium Load scenario had a packet rejection rate of 3.18% while the *Uniform High Load* scenario had no packet rejections. Next, at a low loading level the system performed well despite the failure of satellites or the distribution of traffic. Both the *Uniform Low Load* and the *Non-uniform Low Load* scenarios had no packet rejections with up to seven non-operational satellites. This illustrates the importance of evaluating the network at high loading levels, and supports the results previously obtained by Stenger [Ste96]. At a medium loading level, the traffic distribution impacted the network performance more than the failure of satellites. The *Uniform Medium Load* scenario had an acceptable packet rejection rate with up to five non-operational satellites, while the *Non-uniform Medium Load* scenario performed unacceptably with a full satellite constellation. Finally, at a high loading level the system was much more sensitive to the failure of satellites. The *Uniform High Load* scenario had a packet rejection rate of 1.18% with three non-operational satellites, while the *Uniform Medium Load* had a rejection rate of 2.34% with seven non-operational satellites.

4.5 Analysis of Delay Test Scenarios

The five test scenarios described in Section 4.3 represent different operating conditions for the IRIDIUM® network. The effect of non-operational satellites on both end-to-end delay and packet rejection rate was analyzed for each scenario. For each scenario the end-to-end delay was measured from Kansas City to the six other earth stations. The percent of packets generated that were rejected from the network was also calculated for each scenario. Both of these measurements were made with zero, three, five, and seven non-operational satellites.

4.5.1 Uniform Distribution Low Load

The *Uniform Low Load* scenario had end-to-end delays below the benchmark of 400-ms and no packet rejections with up to seven non-operational satellites. With a full satellite constellation, the end-to-end delay to the various earth stations varied from 98.17-ms to 137.21-ms. With seven non-operational satellites, the delay varied between 160.95-ms and 198.74-ms. The end-to-end delay is plotted against the number of non-operational satellites for each earth station in Figure 15.

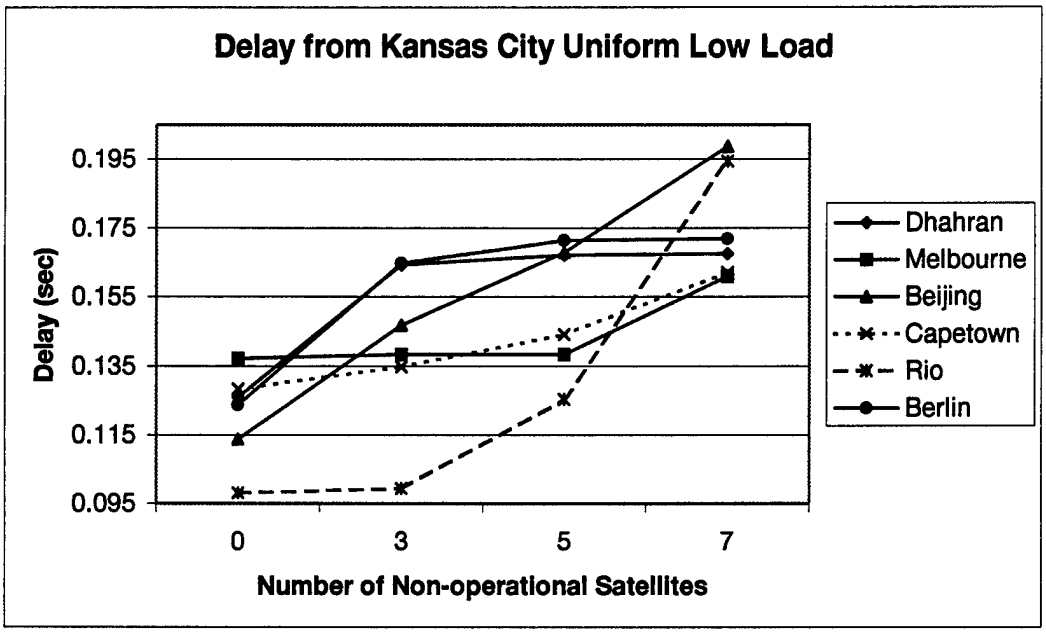

Figure 15: Delay Kansas City to Other Earth Stations Uniform Low Load Scenario

Three of the cities in Figure 15 experienced an increase in end-to-end delay with three non-operational satellites. The other three cities did not have a significant increase in end-to-end delay until either five or seven satellites were non-operational. This indicates that the increase in end-to-end delay resulted primarily from the change in path. Queuing delay did not have a significant impact at this loading level. In this scenario the IRIDIUM® system was able to provide real-time communications despite the non-

operational satellites. The performance in this scenario will be compared with the other scenarios to determine the effect of increasing the traffic load or changing the traffic distribution.

4.5.2 Uniform Distribution Medium Load

The *Uniform Medium Load* Scenario had end-to-end delays below the benchmark of 400-ms with up to seven non-operational satellites and packet rejection rates below the benchmark of 1% with up to five non-operational satellites. With a full satellite constellation, the end-to-end delay varied between 109.36-ms and 152.73-ms. This is an increase of up to 15.52-ms over the maximum delay in the *Uniform Low Load* Scenario with a full satellite constellation. With seven non-operational satellites the end-to-end delay ranged from 213.03-ms to 279.97-ms. This is an increase of up to 81.23-ms above the maximum delay in the *Uniform Low Load* scenario with seven non-operational satellites. The end-to-end delay is plotted against the number of non-operational satellites for each earth station in Figure 16.

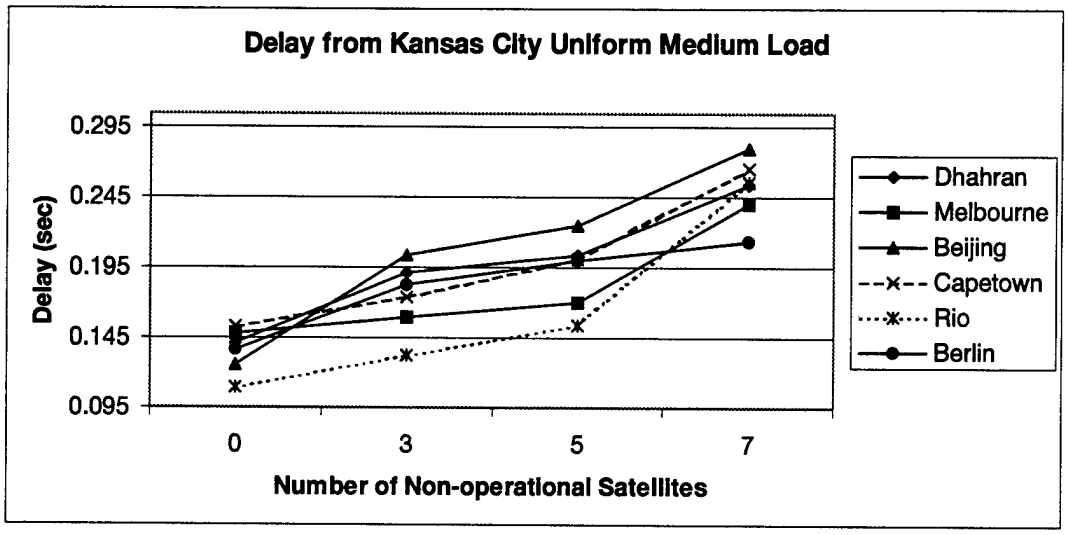

Figure 16: Delay from Kansas City to Other Earth Stations Uniform Medium Load

All six of the cities in Figure 16 experienced an increase in end-to-end delay with three non-operational satellites. The delay increased for each earth station, as more satellites become non-operational. This indicates that queuing delay had a significant role and that the increase in delay was not simply the result of a changing path. There were no packet rejections with zero or three non-operational satellites. The packet rejection rate was 0.03% with five non-operational satellites and 2.34% with seven non-operational satellites. In this scenario the IRIDIUM® system was able to provide real-time communications with up to five non-operational satellites.

4.5.3 Uniform Distribution High Load

The *Uniform High Load* scenario had end-to-end delays below the benchmark of 400-ms with up to seven non-operational satellites and packet rejection rates below the benchmark of 1% with a full satellite constellation. The end-to-end delay ranged from 124.19-ms to 211.53-ms with a full satellite constellation. This is an increase of up to 74.32-ms over the maximum delay for the *Uniform Low Load* scenario with a full satelliteconstelation. The end-to-end delay varied between 229.76-ms and 281.01-ms with seven non-operational satellites. This is an increase of up to 82.27-ms over the Uniform Low Load scenario with seven non-operational satellites. The end-to-end delay is plotted against the number of non-operational satellites for all earth stations in Figure 17. Most of the cities in Figure 17 experienced an increase in end-to-end delay with three non-operational satellites. However, the delay leveled off for three of the cities with five and seven non-operational satellites. This indicates that the network was experiencing packet rejections.

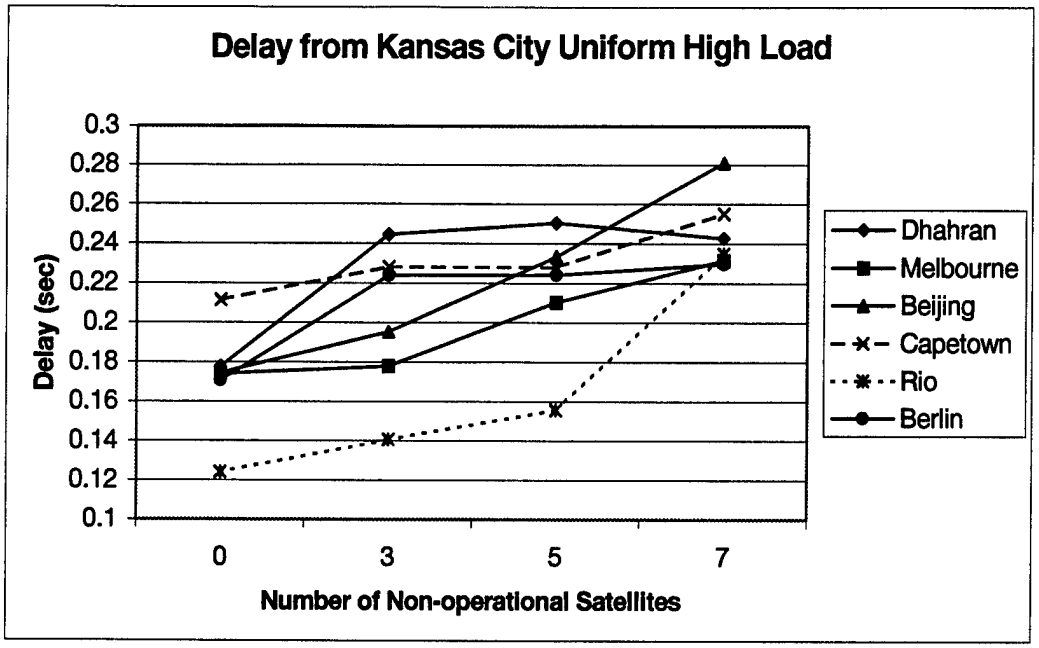

Figure 17: Delay from Kansas City to Other Earth Stations Uniform High Load

The packets between Kansas City and these cities that had delays in excess of 400-ms were being rejected and the mean end-to-end packet delay did not increase. The packet rejection rate with three non-operational satellites was 1.18% and it increased to 5.34% with seven non-operational satellites. In this scenario, the IRIDIUM® system is only able to provide real-time communications with a full satellite constellation.

4.5.4 Non-uniform Distribution Low Load

The *Non-uniform Low Load* scenario had end-to-end delays below the benchmark of 400-ms and no packet rejections with up to seven non-operational satellites. The end-to-end delay ranged from 111.36-ms to 151.46-ms with a full satellite constellation. This is an increase of up to 14.25-ms over the maximum delay for the Uniform Low Load scenario with a full satellite constellation. The end-to-end delay varied between 202.68-ms and 260.65-ms with seven non-operational satellites. This is an increase of up to

61.91-ms over the Uniform Low Load scenario with seven non-operational satellites. The end-to-end delay is plotted against the number of non-operational satellites for all earth stations in Figure 18.

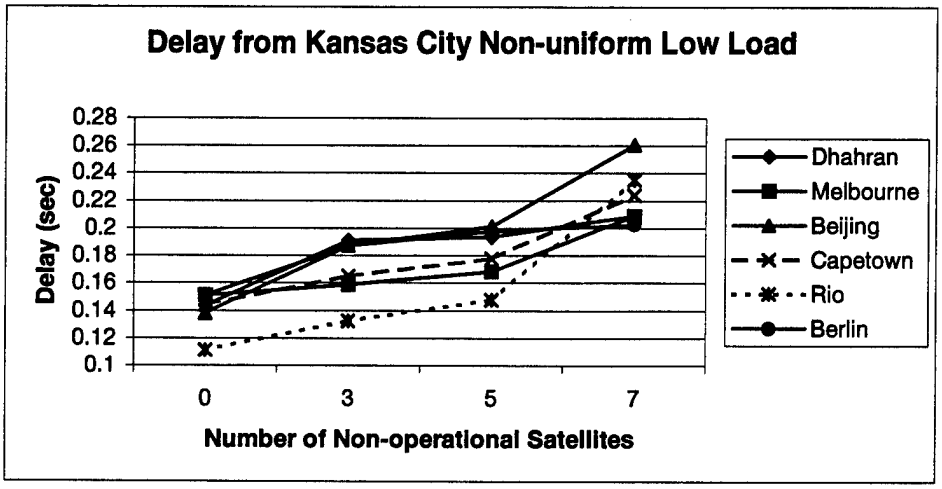

Figure 18: Delay from Kansas City to Other Earth Stations Non-uniform Low Load

Each of the cities in Figure 18 experienced an increase in end-to-end delay with three non-operational satellites. This indicates that queuing delay is affecting the end-to-end delay for all cities. Despite the fact that this scenario had a high volume of traffic between Kansas City and Dhahran, the end-to-end delay to Dhahran was not the highest of all the cities. This was due to the fact that the network was operating at a low loading level. In this scenario the IRIDIUM® system was able to provide real-time communications with up to seven non-operational satellites.

4.5.5 Non-Uniform Distribution Medium Load

The *Non-uniform Medium Load* scenario had end-to-end delays below the benchmark of 400-ms with up to seven non-operational satellites, but was the only scenario that rejected packets with a full satellite constellation. The end-to-end delay ranged from 134.13-ms to 207.12-ms with a full satellite constellation. This is an

increase of up to 69.91-ms over the maximum delay for the Uniform Low Load scenario with a full satellite constellation. The end-to-end delay varied between 214.88-ms and 299.57-ms with seven non-operational satellites. This is an increase of up to 100.83-ms over the Uniform Low Load scenario with seven non-operational satellites. The end-to-end delay for each of the earth stations is plotted against the number of non-operational satellites in Figure 19.

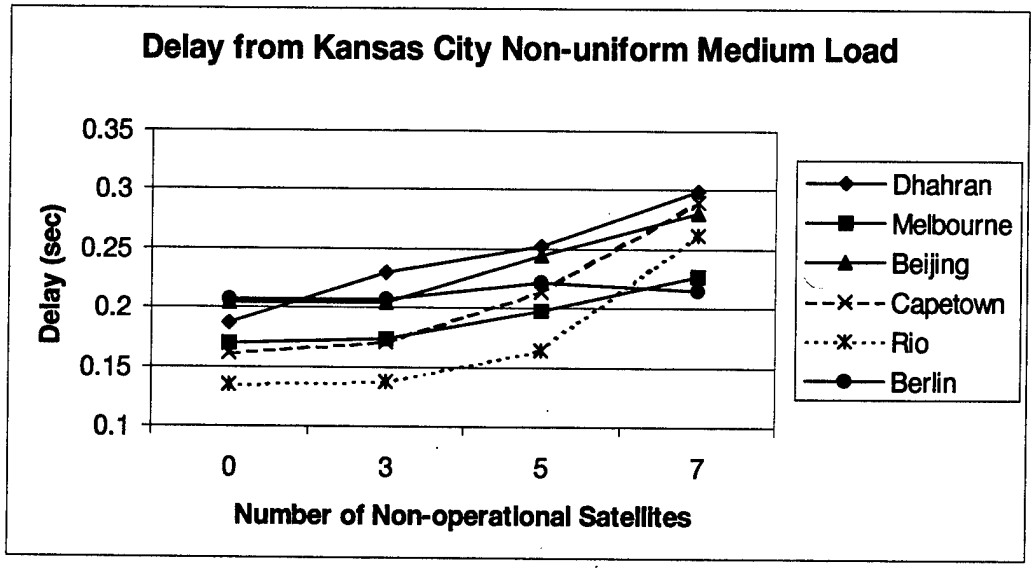

Figure 19: Delay from Kansas City to Other Earth Stations Non-uniform Medium Load

The end-to-end delay for most of the cities in Figure 19 increased as the number of non-operational satellites increased. The end-to-end delay between Kansas City and Dhahran was higher than that between Kansas City and any other earth station with three to seven non-operational satellites. At this loading level, the high traffic link between Kansas City and Dhahran experienced significant queuing delay. The packet rejection rates in this scenario ranged from 3.18% with a full satellite constellation to 8.98% with seven non-operational satellites. As a result of both the non-uniform traffic distribution and medium

traffic load, this scenario was not able to meet the real-time voice traffic benchmark of 1% packet rejection.

4.6 Network Access Test Scenarios

The analysis of an earth station's ability to access the IRIDIUM® network was conducted with two different scenarios. The scenarios represent different earth stations since the average number of satellites visible changes with the latitude of the earth station. Each of the test scenarios was run with zero, three, five, and seven non-operational satellites. The access tests used the same non-operational satellites as the delay tests. Up to this point in the chapter, the analysis has focused on the effect of non-operational satellites on end-to-end delay and packet rejection rate under the assumption that the earth station could access the network. Now, the focus shifts to an earth station's ability to access the network over a period of 24-hours. The period of 24-hours was selected because the earth stations and the satellite constellation are in the same relative position approximately every 24-hours. An earth station sees each IRIDIUM® satellite twice each day. One time it will be travelling from North to South, and the other time from South to North.

4.6.1 Equatorial City

The *Equatorial City* scenario models the visibility of satellites over time from a location directly on the equator. Since the IRIDIUM® orbits are near-polar, the distance between satellites in adjacent orbital planes is the largest when they are over the equatorial region. The larger separation between satellites causes the earth stations at the equator to have fewer visible satellites. In this respect the *Equatorial City* scenario

serves as a baseline in the visibility analysis. The failure of satellites will have a greater effect on an equatorial city than on a city located at higher or lower latitudes.

4.6.2 North American City

The *North American City* scenario models the visibility of satellites over time from Kansas City. This provides a visibility analysis for a typical city in the Northern Hemisphere. Because of the symmetric nature of the IRIDIUM® satellite constellation, the results of this scenario can also provide a visibility analysis for a typical city in the Southern Hemisphere.

4.7 Analysis of Network Access Performance Metrics

The performance metrics used to analyze the network access in each scenario were the average number of visible satellites, the cumulative outage time, and the maximum outage time as defined in Sections 3.10.3, 3.10.4, and 3.10.5 respectively.

4.7.1 Analysis of Average Number of Visible Satellites

The average number of satellites visible over a 24-hour period ranged from 1.15 to 1.69. The *Equatorial City* scenario with seven non-operational satellites had the lowest average visibility, and the *North American City* with a full satellite constellation had the highest average visibility. The average number of visible satellites for each scenario is plotted against the number of non-operational satellites in Figure 20. Figure 20 shows that in both scenarios the average number of visible satellites decreased at approximately the same rate when the number of non-operational satellites was increased. It also shows that the *North American City* had a higher average number of visible satellites with seven non-operational satellites than the *Equatorial City* had with a full

satellite constellation. This illustrates that a user's location has a more significant impact on his ability to access the network than does the failure of satellites.

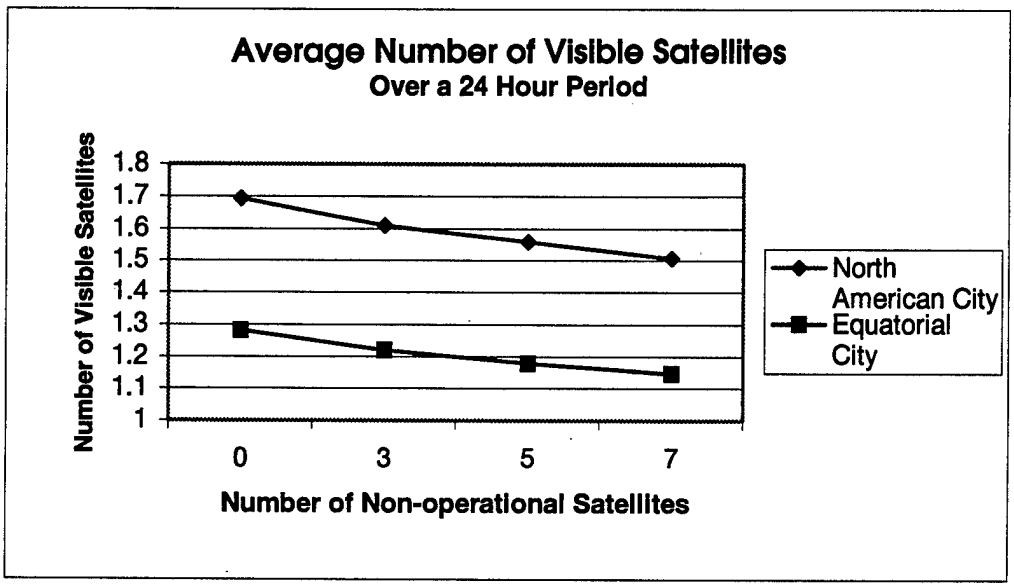

Figure 20: Average Number of Visible Satellites by Scenario

4.7.2 Analysis of Cumulative Outage Time

The cumulative outage time over a 24-hour period ranged from a low of zero minutes to a high of 120-minutes across all test scenarios. As discussed in Section 3.10.4, the IRIDIUM® system is designed to have continuous whole earth coverage. Both the *Equatorial City* scenario and the *North American City* scenario had no outage time with a full satellite constellation. The *Equatorial City* scenario with seven non-operational satellites had the longest cumulative outage of 120-minutes in a 24-hour period. The cumulative outage time as a function of the number of non-operational satellites is plotted in Figure 21. The *North American City* experienced significantly lower cumulative outage times because it had a larger average number of visible satellites. The *Equatorial City* experienced cumulative outage times longer than the

North American City by 17-minutes and 40-minutes with three and seven non-operational satellites respectively.

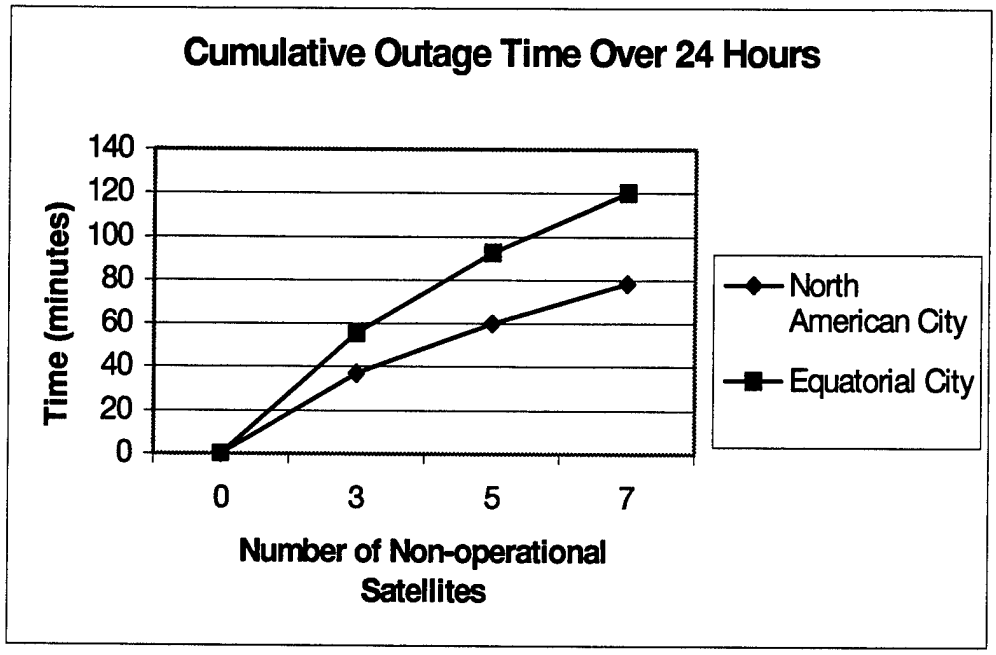

Figure 21: Cumulative Outage Time by Scenario

The *Equatorial City* slightly exceeded the benchmark of 55.41-minutes cumulative outage time with three non-operational satellites. The *North American City* exceeded the same benchmark with five non-operational satellites.

4.7.3 Analysis of Maximum Continuous Outage Time

The maximum continuous outage time over a 24-hour period ranged from a low of zero minutes to a high of 25.43-minutes. As discussed in Section 3.10.4, the IRIDIUM® system is designed to have continuous whole earth coverage. Both the *Equatorial City* and the *North American City* scenarios had no outages with a full satellite constellation. The *Equatorial City* scenario with seven non-operational satellites had the longest outage time of 25.43-minutes. The maximum outage time for each scenario is plotted as a function of non-operational satellites in Figure 22.

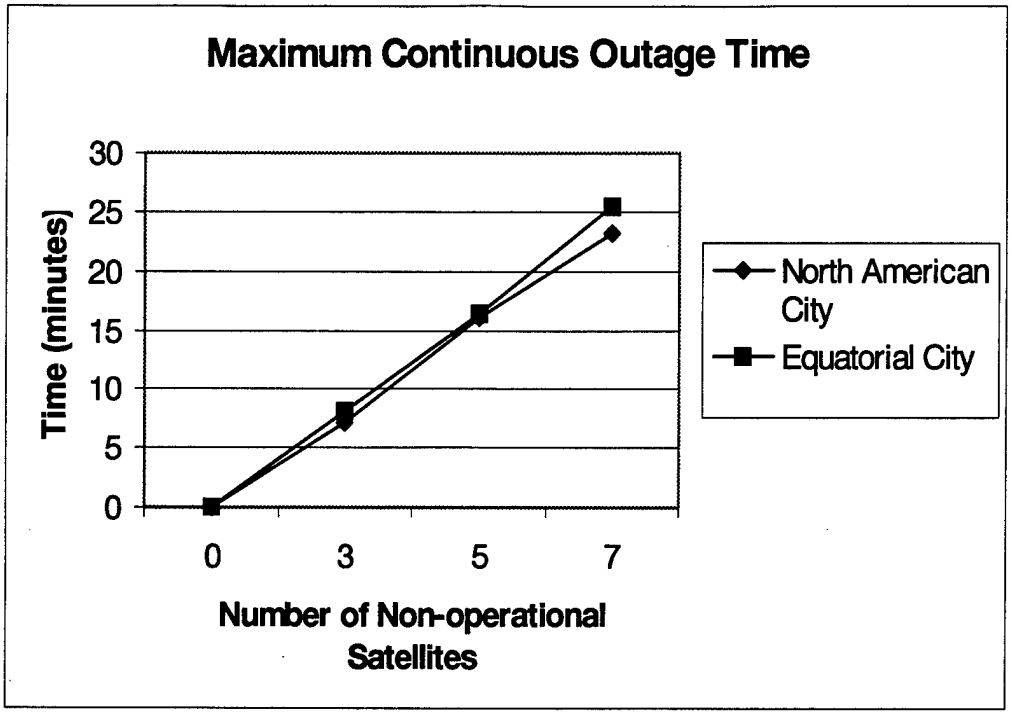

Figure 22: Maximum Continuous Outage Time by Scenario

The *North American City* and the *Equatorial City* experienced similar maximum outage times for each number of non-operational satellites. This indicates that the number of non-operational satellites has a more significant impact on the maximum outage time than the earth station location does. Both the *North American City* and the *Equatorial City* exceeded the benchmark of 12.04-minutes with 5 non-operational satellites.

4.8 Analysis of Network Access Test Scenarios

The scenarios defined in Section 4.6 have different abilities to access the IRIDIUM® network based upon the earth station geographical location. For each scenario, the average number of satellites, cumulative outage time, and maximum outage time were analyzed. The measurements were made for zero, three, five, and seven satellites in each case.

4.8.1 Equatorial City

The *Equatorial City* scenario had between one and three satellites visible with a full satellite constellation. The percent of time that each number of satellites was visible over a 24-hour period is plotted in Figure 23.

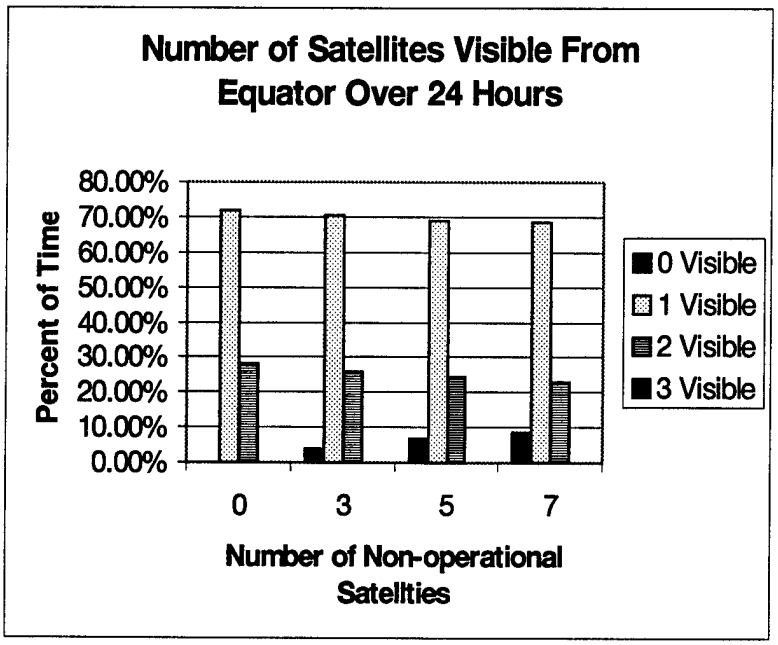

Figure 23: Percent of Time Satellites Are Visible from Equator

The *Equatorial City* had one visible satellite over 68% of the time and two visible satellites less than 28% of the time regardless of the number of non-operational satellites. Three satellites were visible less than 0.05% of the time. The network access results for this scenario are given in Table 12.

Table 12: Network Access Results for Equatorial City Scenario

Equator	Number of Non-operational Satellites			
	0	3	5	7
Average Number of Satellites Visible	1.28	1.22	1.18	1.15
Cumulative Outage Time (min.)	0.00	55.43	92.83	120.00
Maximum Continuous Outage Time (min)	0.00	8.04	16.30	25.43

The results in Table 12 show that this scenario was able to meet the maximum continuous outage time benchmark of 12.04-minutes with up to 3 non-operational The *Equatorial City* scenario exceeded .the cumulative outage time benchmark of 55.41-minutes with only three non-operational satellites.

4.8.2 North American City

The *North American City* had from 1 to 4 satellites visible with a full satellite constellation. The percent of time that each number of satellites was visible is shown in Figure 24.

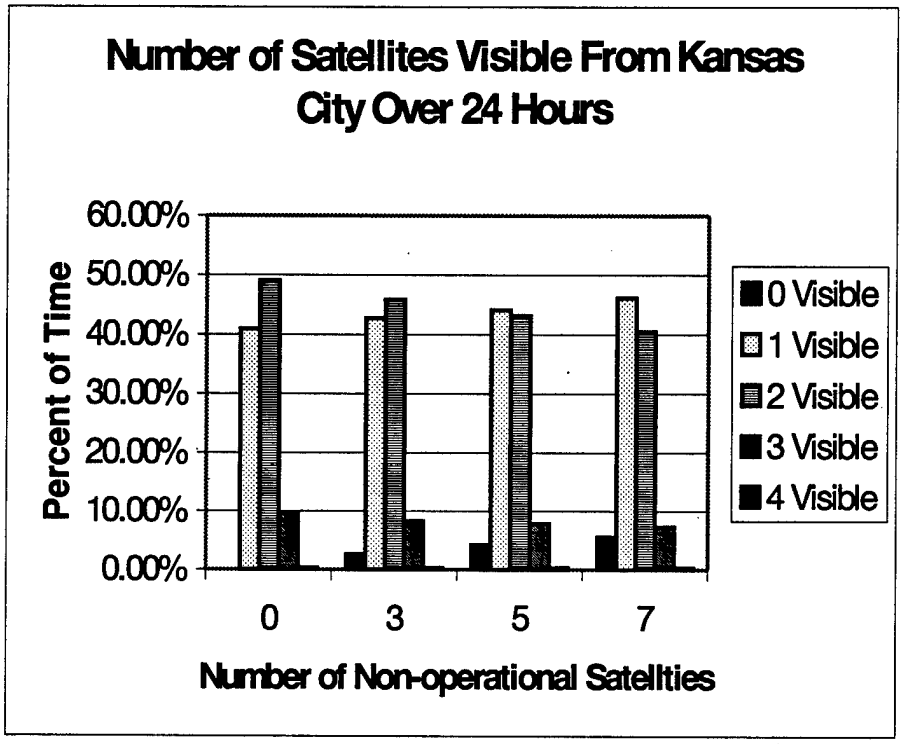

Figure 24: Percent of Time Satellites are Visible From Kansas City

The *North American* scenario had one satellite visible over 40% of the time and two satellites visible over 40% of the time regardless of the number of non-operational satellites. The network access results for this scenario are given in Table 13.

Table 13: Network Access Results for North American City Scenario

Kansas City	Number of Non-operational Satellites			
	0	3	5	7
Average Number of Satellites Visible	1.69	1.61	1.56	1.51
Cumulative Outage Time (min.)	0.00	36.96	59.78	78.26
Maximum Continuous Outage Time (min)	0.00	7.17	16.09	23.26

This scenario was able to meet both the cumulative outage time benchmark of 55.14-minutes and the maximum continuous outage time benchmark of 12.04-minutes with up to 3 non-operational satellites.

4.9 Summary of Analysis

Both the delay analysis presented in Sections 4.3 to 4.5 and the network access analysis presented in Sections 4.6 to 4.8 demonstrated that the IRIDIUM® system is able to meet real-time communications constraints with a number of non-operational satellites. In the delay analysis, both the loading level and the traffic distribution had a significant impact on the system's ability to perform with non-operational satellites. The *Non-uniform Medium Load* scenario had a packet rejection rate of 3.18% with a full constellation. The scenario also had the highest rejection rate of 8.98% with seven non-operational satellites. The Uniform High Load Scenario was the next most sensitive to satellite failures with a packet rejection rate of 1.18% for three non-operational satellites. The delay analysis demonstrated the importance of analyzing the IRIDIUM® system at high loading levels and non-uniform traffic distributions. Since only one non-uniform traffic distribution was used in this research, future research in this area could examine other traffic distributions. The network access analysis demonstrated that non-operational satellites have a significant impact on a user's ability to access the network. The delay analysis showed that the IRIDIUM® system met real-time communications

constraints at low loading levels with up to seven non-operational satellites. However, the network access analysis revealed that a user's ability to access the network is significantly degraded with three to five non-operational satellites. This illustrated the importance of analyzing both the delay and the network access as the number of non-operational satellites increases.

CHAPTER 5

CONCLUSIONS AND RECOMMENDATIONS

5.1 Restatement of Research Goal

The goal of this research was to assess the IRIDIUM® Low Earth Orbit (LEO) satellite network's capability to provide real-time communications with a degraded satellite constellation.

5.2 Conclusions

The IRIDIUM® LEO satellite network is a robust network that is capable of providing real-time voice communications with multiple non-operational satellites. The ability of the system to meet the end-to-end delay benchmark of 400-ms and packet rejection rate benchmark of 1% depends upon both the loading level and traffic distribution. With a low loading level, the IRIDIUM® network met both benchmarks with seven non-operational satellites regardless of the traffic distribution. For a medium loading level, the system met both benchmarks with five non-operational satellites and a uniform traffic distribution. A medium loading level with a non-uniform traffic distribution exceeded the packet rejection rate benchmark with a full satellite constellation. A high loading level with a uniform traffic distribution exceeded the packet rejection rate benchmark with three non-operational satellites.

The ability of the IRIDIUM® network to meet the network access benchmarks of cumulative outage time less than 55.41-minutes and maximum continuous outage time less than 12.04-minutes was dependent upon the earth stations location. An earth station at the equator met the maximum continuous outage time benchmark with three non-

operational satellites. However, the scenario only met the cumulative outage time benchmark with a full satellite constellation. A typical North American city met both benchmarks with three non-operational satellites.

The robustness of the IRIDIUM® network was demonstrated by selecting critical satellites to fail. The non-operational satellites were selected in each scenario by algorithmically determining the most heavily utilized satellites. From this respect, the results represent a worst case scenario. The results of a similar delay analysis and network access analysis with randomly failing satellites should result in better network performance.

5.3 Significant Results of Research

There is currently a lack of openly published literature in the area of LEO satellite network survivability. The most recent work by Stenger demonstrated that IRIDIUM® was a robust network, but was limited to an analysis at low loading levels due to long simulation run times [Ste96]. One of the most significant contributions of this research was the analysis of the IRIDIUM® network at high loading levels. By appropriately scaling modeled network parameters, as discussed in Section 3.6, this research overcame the simulation run-time limitations that constrained Stenger's work. Another significant result of this research was the analysis of an earth station's ability to access the IRIDIUM® network with a degraded satellite constellation. Previous work focused only on the delay performance [Ste96]. The combination of analyzing the network at high loading levels and analyzing an earth station's ability to access the network provided a more complete assessment of how the IRIDIUM® system performs with a degraded

satellite constellation. The results of this research are summarized in three technical papers submitted for publication [FoR98a, FoR98b, FoR98c].

5.4 Recommendations for Future Research

There are three primary areas in which this research can be expanded. The first area is the analysis of different non-uniform traffic distributions. This research used a non-uniform traffic distribution that created a high traffic link between two cities. The significant impact that this had on network performance indicates the need to analyze the effect of other non-uniform traffic distributions. The next area is the analysis of different routing algorithms. Since the actual routing algorithm of the IRIDIUM® system is unpublished, this analysis used a simple Dijkstra routing algorithm. It is likely that the actual routing algorithm has the capability to balance the network load and route around congested satellites. The significant effect that increasing the loading had on network performance indicates the need to analyze more complicated routing algorithms. The third area is the analysis of other LEO satellite constellations such as Globalstar. Globalstar uses fewer satellites at a higher altitude than the IRIDIUM® satellites. This results in longer in-view times for individual satellites and larger satellite coverage areas. The significant effect that non-operational satellites had on a user's ability to access the IRIDIUM® satellite network indicates the need to analyze other satellite constellations in a similar manner.

APPENDIX

This Appendix contains the tabulated end-to-end delay results and 95% confidence intervals for each test scenario. The results for the *Uniform Low Load* scenario with a full satellite constellation and the *Non-uniform Medium Load* scenario with seven non-operational satellites are presented in Section 4.2

Table 14: Results for Uniform Low Load with Three Non-operational Satellites

From Kansas City to:	Average Sample Mean	Standard Deviation	95% Confidence Interval	
			Minimum	Maximum
Dhahran	0.16432	0.00023	0.16432	0.00023
Melbourne	0.13837	0.00028	0.13837	0.00028
Beijing	0.14688	0.00042	0.14688	0.00042
Capetown	0.13480	0.00143	0.13480	0.00143
Rio	0.09945	0.00044	0.09945	0.00044
Berlin	0.16476	0.00011	0.16476	0.00011

Table 15: Results for Uniform Low Load with Five Non-operational Satellites

From Kansas City to:	Average Sample Mean	Standard Deviation	95% Confidence Interval	
			Minimum	Maximum
Dhahran	0.16707	0.00014	0.16673	0.16741
Melbourne	0.13839	0.00029	0.13767	0.13911
Beijing	0.16783	0.00046	0.16670	0.16896
Capetown	0.14417	0.00108	0.14147	0.14686
Rio	0.12549	0.00031	0.12471	0.12627
Berlin	0.17135	0.00016	0.17095	0.17175

Table 16: Results for Uniform Low Load with Seven Non-operational Satellites

From Kansas City to:	Average Sample Mean	Standard Deviation	95% Confidence Interval	
			Minimum	Maximum
Dhahran	0.16707	0.00014	0.16673	0.16741
Melbourne	0.13839	0.00029	0.13767	0.13911
Beijing	0.16783	0.00046	0.16670	0.16896
Capetown	0.14417	0.00108	0.14147	0.14686
Rio	0.12549	0.00031	0.12471	0.12627
Berlin	0.17135	0.00016	0.17095	0.17175

Table 17: Results for Uniform Medium Load with a Full Satellite Constellation

From Kansas City to:	Average Sample Mean	Standard Deviation	95% Confidence Interval	
			Minimum	Maximum
Dhahran	0.14077	0.00170	0.13654	0.14500
Melbourne	0.14794	0.00181	0.14343	0.15245
Beijing	0.12627	0.00257	0.11989	0.13264
Capetown	0.15273	0.00242	0.14673	0.15874
Rio	0.10936	0.00114	0.10654	0.11218
Berlin	0.13631	0.00308	0.12867	0.14396

Table 18: Results for Uniform Medium Load with Three Non-operational Satellites

From Kansas City to:	Average Sample Mean	Standard Deviation	95% Confidence Interval	
			Minimum	Maximum
Dhahran	0.19176	0.00183	0.18722	0.19630
Melbourne	0.15984	0.00167	0.15569	0.16400
Beijing	0.20378	0.00153	0.19997	0.20760
Capetown	0.17435	0.00668	0.15775	0.19095
Rio	0.13281	0.00088	0.13061	0.13501
Berlin	0.18300	0.00071	0.18123	0.18478

Table 19: Results for Uniform Medium Load with Five Non-operational Satellites

From Kansas City to:	Average Sample Mean	Standard Deviation	95% Confidence Interval	
			Minimum	Maximum
Dhahran	0.20382	0.00071	0.20206	0.20559
Melbourne	0.17002	0.00214	0.16470	0.17535
Beijing	0.22494	0.00169	0.22074	0.22914
Capetown	0.20104	0.00072	0.19926	0.20282
Rio	0.15372	0.00886	0.13170	0.17574
Berlin	0.20000	0.00171	0.19574	0.20426

Table 20: Results for Uniform Medium Load with Seven Non-operational Satellites

From Kansas City to:	Average Sample Mean	Standard Deviation	95% Confidence Interval	
			Minimum	Maximum
Dhahran	0.25398	0.00166	0.24986	0.25811
Melbourne	0.24036	0.00427	0.22975	0.25097
Beijing	0.27997	0.00366	0.27087	0.28908
Capetown	0.26539	0.00052	0.26409	0.26670
Rio	0.25556	0.00897	0.23327	0.27784
Berlin	0.21303	0.00124	0.20994	0.21612

Table 21: Results for Uniform High Load with a Full Satellite Constellation

From Kansas City to:	Average Sample Mean	Standard Deviation	95% Confidence Interval	
			Minimum	Maximum
Dhahran	0.17777	0.00627	0.16219	0.19334
Melbourne	0.17408	0.00052	0.17278	0.17538
Beijing	0.17467	0.00403	0.16465	0.18468
Capetown	0.21153	0.01893	0.16449	0.25857
Rio	0.12419	0.00158	0.12028	0.12811
Berlin	0.17070	0.00219	0.16526	0.17614

Table 22: Results for Uniform High Load with Three Non-operational Satellites

From Kansas City to:	Average Sample Mean	Standard Deviation	95% Confidence Interval	
			Minimum	Maximum
Dhahran	0.24435	0.00656	0.22806	0.26063
Melbourne	0.17803	0.00061	0.17652	0.17954
Beijing	0.19527	0.00034	0.19442	0.19611
Capetown	0.22812	0.00938	0.20482	0.25143
Rio	0.14062	0.00234	0.13480	0.14645
Berlin	0.22388	0.00099	0.22142	0.22633

Table 23: Results for Uniform High Load with Five Non-operational Satellites

From Kansas City to:	Average Sample Mean	Standard Deviation	95% Confidence Interval	
			Minimum	Maximum
Dhahran	0.25044	0.00102	0.24792	0.25296
Melbourne	0.21024	0.00104	0.20766	0.21281
Beijing	0.23334	0.00150	0.22963	0.23705
Capetown	0.22812	0.00454	0.21684	0.23940
Rio	0.15572	0.00230	0.14872	0.16273
Berlin	0.22428	0.00241	0.21829	0.23027

Table 24: Results for Uniform High Load with Seven Non-operational Satellites

From Kansas City to:	Average Sample Mean	Standard Deviation	95% Confidence Interval	
			Minimum	Maximum
Dhahran	0.24272	0.00480	0.23080	0.25464
Melbourne	0.23149	0.00373	0.22223	0.24075
Beijing	0.28101	0.00173	0.27672	0.28530
Capetown	0.25508	0.00632	0.23938	0.27077
Rio	0.23481	0.00866	0.21328	0.25633
Berlin	0.22976	0.00327	0.22163	0.23789

Table 25: Results for Non-uniform Low Load with a Full Satellite Constellation

From Kansas City to:	Average Sample Mean	Standard Deviation	95% Confidence Interval	
			Minimum	Maximum
Dhahran	0.14350	0.00041	0.14248	0.14453
Melbourne	0.15138	0.00129	0.14818	0.15458
Beijing	0.13803	0.00145	0.13444	0.14163
Capetown	0.14391	0.00215	0.13856	0.14927
Rio	0.11136	0.00081	0.10934	0.11338
Berlin	0.15146	0.00108	0.14878	0.15413

Table 26: Results for Non-uniform Low Load with Three Non-operational Satellites

From Kansas City to:	Average Sample Mean	Standard Deviation	95% Confidence Interval	
			Minimum	Maximum
Dhahran	0.19123	0.00070	0.18948	0.19298
Melbourne	0.15892	0.00101	0.15640	0.16144
Beijing	0.18706	0.00167	0.18290	0.19122
Capetown	0.16531	0.00197	0.16042	0.17020
Rio	0.13244	0.00162	0.12842	0.13647
Berlin	0.18740	0.00050	0.18616	0.18864

Table 27: Results for Non-uniform Low Load with Five Non-operational Satellites

From Kansas City to:	Average Sample Mean	Standard Deviation	95% Confidence Interval	
			Minimum	Maximum
Dhahran	0.19378	0.00158	0.18985	0.19770
Melbourne	0.16858	0.00074	0.16673	0.17043
Beijing	0.20140	0.00438	0.19052	0.21229
Capetown	0.17811	0.00467	0.16650	0.18972
Rio	0.14772	0.00147	0.14406	0.15137
Berlin	0.19794	0.00096	0.19555	0.20033

Table 28: Results for Non-uniform Low Load with Seven non-operational Satellites

From Kansas City to:	Average Sample Mean	Standard Deviation	95% Confidence Interval	
			Minimum	Maximum
Dhahran	0.20897	0.00592	0.19426	0.22367
Melbourne	0.20904	0.00770	0.18991	0.22816
Beijing	0.26065	0.00763	0.24170	0.27960
Capetown	0.22409	0.00255	0.21776	0.23041
Rio	0.23515	0.00439	0.22425	0.24605
Berlin	0.20268	0.00151	0.19894	0.20643

Table 29: Results for Non-uniform Medium Load with a Full Satellite Constellation

From Kansas City to:	Average Sample Mean	Standard Deviation	95% Confidence Interval	
			Minimum	Maximum
Dhahran	0.18725	0.00371	0.17804	0.19646
Melbourne	0.16924	0.00038	0.16829	0.17019
Beijing	0.20404	0.00126	0.20090	0.20718
Capetown	0.16085	0.00102	0.15831	0.16339
Rio	0.13413	0.00121	0.13113	0.13714
Berlin	0.20712	0.00509	0.19448	0.21976

Table 30: Results for Non-uniform Medium Load with Three Non-operational Satellites

From Kansas City to:	Average Sample Mean	Standard Deviation	95% Confidence Interval	
			Minimum	Maximum
Dhahran	0.23030	0.00296	0.22294	0.23765
Melbourne	0.17343	0.00081	0.17141	0.17544
Beijing	0.20391	0.00410	0.19373	0.21408
Capetown	0.17095	0.00208	0.16577	0.17613
Rio	0.13716	0.00259	0.13073	0.14360
Berlin	0.20636	0.00084	0.20427	0.20844

Table 31: Results for Non-uniform Medium Load with Five Non-operational Satellites

From Kansas City to:	Average Sample Mean	Standard Deviation	95% Confidence Interval	
			Minimum	Maximum
Dhahran	0.25220	0.00209	0.24701	0.25740
Melbourne	0.19768	0.00089	0.19546	0.19989
Beijing	0.24467	0.00422	0.23419	0.25516
Capetown	0.21428	0.00392	0.20454	0.22401
Rio	0.16386	0.00136	0.16048	0.16724
Berlin	0.22183	0.00123	0.21877	0.22489

BIBLIOGRAPHY

[Ada87] Adams, W. S. and Rider, L., "Circular Polar Constellations Providing Continuous Single or Multiple Coverage Above a Specified Latitude," *The Journal of Astronautical Sciences*, Vol. 35, No. 2 April-June 1987, pp. 155-192.

[Ana95] Ananaso, Fulvio and Priscolli, Francesco, "The Role of Satellites in Personal Communication Services," *IEEE Journal on Selected Areas in Communications*, Vol. 13, No. 2, February 1995, pp. 180-195.

[Bru96] P Brunt, "IRIDIUM® - Overview and Status," *Space Communications*, Vol. 14, No. 2, 1996, pp. 61-68.

[Cad95] BoNES SATLAB User's Guide, Cadence Design Systems, Incorporated, June 1995.

[Com93] Gary M. Comparetto, "A Technical Comparison of Several Global Mobile Satellite Communications Systems," *Space Communications*, Vol. 11, No. 2, 1993, pp. 97-104.

[Dol93] Dolan, Alan and Aldous, Joan, Networks and Algorithms, an Introductory Approach, John Wiley & Sons, New York, 1993, pp. 126-140.

[FoR98a] Fossa, Carl E., Raines, Richard A., Gunsch, Gregg H., and Temple, Michael A., "A Performance Analysis of the IRIDIUM® Low Earth Orbit Satellite System," *ACM/IEEE International Conference on Mobile Computing and Networks*, 1998 (submitted for publication).

[FoR98b] Fossa, Carl E., Raines, Richard A., Gunsch, Gregg H., and Temple, Michael A., "An Overview of the IRIDIUM® Low Earth Orbit Satellite System," *IEEE National Aerospace and Electronics Conference*, 1998 (submitted for publication).

[FoR98c] Fossa, Carl E., Raines, Richard A., Gunsch, Gregg H., and Temple, Michael A., "A Performance Analysis of the IRIDIUM® Low Earth Orbit Satellite System with a Degraded Satellite Constellation," *ACM Mobile Computing and Communications Review*, 1998 (submitted for publication).

[Gag84] Gagliardi, Robert M., Satellite Communications, Lifetime Learning Publications, Belmont, CA, 1984 pp. 11-17.

[Gan93] Ganz, Aura, Li, Bo, and Gong, Yebin, "Performance Study of Low Earth Orbit Satellite Systems," *IEEE International Conference on Communications*, Vol. 2, 1993, pp. 1098-1102.

[Gea96] Geaghan, Bernard and Yuan, Raymond, "Communications to High Latitudes Using Commercial Low Earth Orbit Satellites," *Proceedings of the 1996 Tactical Communications Conference*, pp. 407-415.

[Hub97] Yvette C. Hubbel, "A Comparison of the Iridium and AMPS Systems," *IEEE Network*, Vol. 11, No. 2, March/April 1997, pp. 52-59.

[Kel96] Keller, Harald and Salzwedel, Horst, "Link Strategy for the Mobile Satellite System Iridium,"*1996 IEEE 46th Vehicular Technology Conference*, Vol. 2, pp. 1220-1224.

[Jai91] Jain, Raj, The Art of Computer Systems Performance Analysis, John Wiley and Sons, Inc., New York, 1991 pp. 30-33.

[New91] Newport, Kris T., and Varshney, Pramond, "Design of Survivable Communications Networks under Performance Constraints," *IEEE Transactions on Reliability*, Vol. 40 No. 4, October 1991, p. 433-440.

[Rai91] Rai, Suresh, and Soh, Sieteng, "A Computer Approach for Reliability Evaluation of Telecommunication Networks with Heterogeneous Link-Capacities," *IEEE Transactions on Reliability*, Vol. 40 No. 4, October 1991, p. 441-451

[Saa94] Tarek N. Saadawi and Mostafa H. Ammar, Fundamentals in Telecommunication Networks, John Wiley and Sons, New York, 1994, p. 25.

[Skl88] Bernard Sklar, Digital Communications Fundamentals and Applications, Prentice Hall, NJ, 1988, pp. 507-526.

[Ste96] Stenger, Douglas K., *Survivability Analysis of the Iridium Low Earth Orbit Satellite Network*, Master's Thesis, School of Electrical Engineering, Air Force Institute of Technology, 1996.

[Vat95] Franceso Vatalaro, Giovanni Emanuele Corazza, Carlo Caini and Carlo Ferrarelli, "Analysis of LEO, MEO, and GEO Global Mobile Satellite Systems in the Presence of Interference and Fading," *IEEE Journal on Selected Areas in Communications*, Vol. 13, No. 2, February 1995, pp. 291-300.

[Wer95] Werner, Markus, Jahn, Axel and Lutz, Erich, "Analysis of System Parameters for LEO/ICO Satellite Communications Networks," *IEEE Journal on Selected Areas in Communications*, Vol. 13, No. 2, February 1995, pp. 371-381.

VITA

Major Carl E. Fossa, Jr. was born on May 11, 1965 in Salem, Massachusetts. He graduated from the United States Military Academy in West Point, New York in 1987 with a Bachelor of Science degree in electrical engineering. Upon graduation, he was commissioned in the U.S. Army Signal Corps. From 1988 to 1990 Major Fossa served as a Platoon Leader in the 67th Signal Battalion, Fort Gordon, Georgia. He was an Assistant Operations Officer in the 67th Signal Battalion from 1990 to 1992 in Fort Gordon, Georgia and Dhahran, Saudi Arabia. In 1993, Major Fossa was assigned as a Systems Engineer, Deputy Chief of Staff, Plans, 5th Signal Command, Worms, Germany. Major Fossa's most recent assignment was as the Commander, 181st Signal Company, 43rd Signal Battalion, Heidelberg, Germany from 1995 to 1996. He entered the Air Force Institute of Technology in 1996 to pursue a Master's of Science degree in electrical engineering. Major Fossa is a graduate of the Signal Officer Basic Course, the Signal Officer Advanced Course, and the Combined Arms and Services Staff School. His awards include the Meritorious Service Medal, Army Commendation Medal with two Oak Leaf Clusters, and Army Achievement Medal.

Permanent Address: 1 Cole St., Beverly, MA 01915

REPORT DOCUMENTATION PAGE

Form Approved
OMB No. 0704-0188

Public reporting burden for this collection of information is estimated to average 1 hour per response, including the time for reviewing instructions, searching existing data sources, gathering and maintaining the data needed, and completing and reviewing the collection of information. Send comments regarding this burden estimate or any other aspect of this collection of information, including suggestions for reducing this burden, to Washington Headquarters Services, Directorate for Information Operations and Reports, 1215 Jefferson Davis Highway, Suite 1204, Arlington, VA 22202-4302, and to the Office of Management and Budget, Paperwork Reduction Project (0704-0188), Washington, DC 20503.

1. AGENCY USE ONLY *(Leave blank)*

2. REPORT DATE
1 Jun 98

3. REPORT TYPE AND DATES COVERED
Thesis

4. TITLE AND SUBTITLE
A Performance Analysis of the Iridium Low Earth Orbit Satellite System

5. FUNDING NUMBERS

6. AUTHOR(S)
Carl E. Fossa, Jr.

7. PERFORMING ORGANIZATION NAME(S) AND ADDRESS(ES)
Air Force Institute of Technology
AFIT/ENG
2950 P St., Bldg. 640
Wright-Patterson AFB, OH 45433-7765

8. PERFORMING ORGANIZATION REPORT NUMBER
AFIT/GE/ENG/98J-01

9. SPONSORING/MONITORING AGENCY NAME(S) AND ADDRESS(ES)
MAJ Michael Shillinger
DCD, Concepts Branch
U.S. Army Signal Center
Fort Gordon, GA 30905 DSN: 780-4210

10. SPONSORING/MONITORING AGENCY REPORT NUMBER

11. SUPPLEMENTARY NOTES

12a. DISTRIBUTION AVAILABILITY STATEMENT
Approved for public release; distribution unlimited.

12b. DISTRIBUTION CODE

13. ABSTRACT *(Maximum 200 words)*

This thesis provides a performance evaluation of the IRIDIUM Low Earth Orbit Satellite system. It examine's the system's ability to meet real-time communications constraints with a degraded satellite constellation. The analysis is conducted via computer simulation. The simulation is run at low, medium, and high loading levels with both uniform and non-uniform traffic distributions. An algorithmic approach is used to select critical satellites to remove from the constellation. Each combination of loading level and traffic distribution is analyzed with zero, three, five and seven non-operational satellites. The measured outputs are ene-to-end packet delay and packet rejection rate. In addition to the delay analysis, a user's ability to access the network with a degraded satellite constellation is evaluated. The average number of visible satellites, cumulative outage time, and maximum continuous outage time are analyzed for both an Equatorial city and a North American city. The results demonstrate that the IRIDIUM network is capable of meeting real-time communication requirements with several non-operational satellites. Both the high loading level and the non-uniform traffic distribution have a significant effect on the network's performance. The analysis of both network delay performance and network access provides a good measure of the overall network performance with a degraded satellite constellation.

14. SUBJECT TERMS
IRIDIUM, Low Earth Orbit Satellite, LEO, satellite communications, mobile communications, network reliability

15. NUMBER OF PAGES
112

16. PRICE CODE

17. SECURITY CLASSIFICATION OF REPORT	18. SECURITY CLASSIFICATION OF THIS PAGE	19. SECURITY CLASSIFICATION OF ABSTRACT	20. LIMITATION OF ABSTRACT
UNCLASSIFIED	UNCLASSIFIED	UNCLASSIFIED	UL